

1-1-2006

Dose comparison of multi-slice computed tomography scanners

James J Kelley
University of Nevada, Las Vegas

Follow this and additional works at: <https://digitalscholarship.unlv.edu/rtds>

Repository Citation

Kelley, James J, "Dose comparison of multi-slice computed tomography scanners" (2006). *UNLV Retrospective Theses & Dissertations*. 2057.
<http://dx.doi.org/10.25669/4jly-0ded>

This Thesis is protected by copyright and/or related rights. It has been brought to you by Digital Scholarship@UNLV with permission from the rights-holder(s). You are free to use this Thesis in any way that is permitted by the copyright and related rights legislation that applies to your use. For other uses you need to obtain permission from the rights-holder(s) directly, unless additional rights are indicated by a Creative Commons license in the record and/or on the work itself.

This Thesis has been accepted for inclusion in UNLV Retrospective Theses & Dissertations by an authorized administrator of Digital Scholarship@UNLV. For more information, please contact digitalscholarship@unlv.edu.

DOSE COMPARISON OF MULTI-SLICE COMPUTED
TOMOGRAPHY SCANNERS

by

James J. Kelley

Bachelor of Science
University of Nevada, Las Vegas
1988

A thesis submitted in partial fulfillment
of the requirements for the

**Master of Science Degree in Health Physics
School of Allied Health Sciences
Division of Health Sciences**

**Graduate College
University of Nevada, Las Vegas
December 2006**

UMI Number: 1441714

INFORMATION TO USERS

The quality of this reproduction is dependent upon the quality of the copy submitted. Broken or indistinct print, colored or poor quality illustrations and photographs, print bleed-through, substandard margins, and improper alignment can adversely affect reproduction.

In the unlikely event that the author did not send a complete manuscript and there are missing pages, these will be noted. Also, if unauthorized copyright material had to be removed, a note will indicate the deletion.

UMI[®]

UMI Microform 1441714

Copyright 2007 by ProQuest Information and Learning Company.

All rights reserved. This microform edition is protected against unauthorized copying under Title 17, United States Code.

ProQuest Information and Learning Company
300 North Zeeb Road
P.O. Box 1346
Ann Arbor, MI 48106-1346



Thesis Approval

The Graduate College
University of Nevada, Las Vegas

_____, 11-16, 2006

The Thesis prepared by

James J. Kelley

Entitled

Dose Comparison of Multi-Slice Computed Tomography Scanners

is approved in partial fulfillment of the requirements for the degree of

Master of Science Degree in Health Physics

Examination Committee Chair

Dean of the Graduate College

Examination Committee Member

Examination Committee Member

Graduate College Faculty Representative

ABSTRACT

Dose Comparison of Multi-Slice Computed Tomography Scanners

by

James J. Kelley

Dr. Phillip Patton, Examination Committee Chair
Associate Professor of Health Physics
University of Nevada, Las Vegas

The rapid technological advances in CT over the past 30 years have resulted in a steady increase in the number of CT scans being performed annually, making it the major source of exposure to the population via diagnostic x-rays. With this increased utilization, the concerns over patient radiation doses from CT have also grown. Although CT studies only amount to about 5% of all X-ray examinations, it contributes approximately 40% of the collective dose from diagnostic radiology to the population. This fact has made CT dosimetry an important topic in diagnostic radiology today. The introduction of multi-slice scanners has focused further attention on this issue; and it is generally believed multi slice scanners can lead to higher patient doses. This is due to the increased abilities of the multi-slice scanners, i.e. increased volume coverage at higher tube currents, which could lead to an increase in patient dose.

This study will provide a comparison of three multi-slice CT scanners. All three scanners are the same make and model and only vary in their slice capabilities. Six protocols are performed, two axial protocols, consisting of one head and one abdomen scan, and four helical protocols, consisting of two head and two abdomen scans. The

acquisition parameters was kept consistent for each set of scans with the goal of providing comparative data to substantiate or refute the concern that multi-slice scanners will increase patient dose.

Doses for all three CT scanners were compared for each protocol. The results showed that the 4-slice CT generated a larger dose than both the 16-slice and the 64-slice scanners. In the axial protocols, the dose decreased as the slice capabilities of the scanners increased. In the helical protocols, the 64-slice scanner produced a larger dose in comparison to the 16-slice scanner.

TABLE OF CONTENTS

ABSTRACT	iii
LIST OF TABLES	vii
LIST OF FIGURES	viii
ACKNOWLEDGEMENTS	ix
CHAPTER 1 INTRODUCTION.....	1
1.1 History of CT.....	1
1.2 Seven Generations of CT	3
1.3 Physics of Helical Scanning.....	9
1.4 Single Slice vs. Multi-Slice	11
1.5 CT Dosimetry	12
CHAPTER 2 METHODS AND MATERIALS	15
2.1 Acquisition Systems	15
2.2 Phantoms	16
2.3 Detector	18
2.4 Scanning Techniques.....	18
2.5 Dose Measurements	21
2.6 Dose Assessment.....	22
CHAPTER 3 RESULTS	27
3.1 Axial Exposure Measurements.....	27
3.2 Helical Exposure Measurements	30
3.3 CTDI _{vol} Results	34
3.4 DLP Results.....	37
3.5 CT Dose Relationship to Pitch	38
3.6 Helical Dose Estimation.....	39
3.7 Effective Dose Results	40
CHAPTER 4 CONCLUSIONS.....	44
4.1 Overall Conclusions	47
4.2 Future Work	48
APPENDIX A CTDI DOSE CALCULATION SHEETS	48
APPENDIX B CTDI HELICAL DOSE ESTIMATION SHEETS.....	67

BIBLIOGRAPHY	71
VITA.....	73

LIST OF TABLES

Table 1.1	Comparison of 4-Slice to Single-Slice CT Scan Times	12
Table 2.1	CT Scanners Technical Specifications	15
Table 2.2	Parameters of 4-Slice Helical CT Scanners	19
Table 2.3	Parameters of 16-Slice Helical CT Scanners	19
Table 2.4	Parameters of 64-Slice Helical CT Scanners	20
Table 2.5	Parameters of 4-Slice Axial CT Scanners	20
Table 2.6	Parameters of 16-Slice Axial CT Scanners	20
Table 2.7	Parameters of 64-Slice Axial CT Scanners	21
Table 3.1	4-Slice Axial Exposure Measurements	28
Table 3.2	16-Slice Axial Exposure Measurements	28
Table 3.3	64-Slice Axial Exposure Measurements	29
Table 3.4	4-Slice Helical Exposure Measurements.....	31
Table 3.5	16-Slice Helical Exposure Measurements.....	32
Table 3.6	64-Slice Helical Exposure Measurements.....	34
Table 3.7	Calculated CTDI _{vol} Comparison Between Exposure and CTDI values	35
Table 3.8	CTDI _{vol} Values for 4, 16, and 64-Slice Scanners	36
Table 3.9	DLP Values for 4, 16, and 64-Slice Scanners	37
Table 3.10	Varying Pitch Effects on Exposure Values	39
Table 3.11	Comparison of CTDI _{vol} Values for Estimated and Actual Helical Scans	40
Table 3.12	Effective Dose Values for 4, 16 and 64-Slice Scanners.....	41

LIST OF FIGURES

Figure 1.1	First Generation CT Scanner	3
Figure 1.2	Ring Artifact	5
Figure 1.3	Third Generation CT Scanner.....	5
Figure 1.4	Helical CT Scanner.....	7
Figure 2.1	CTDI Head and Abdomen Phantoms	14
Figure 2.2	CTDI Dose Calculation Sheet	24

ACKNOWLEDGEMENTS

During the production of this paper, several individuals generously gave their time and expertise to aid in its completion. First, I would like to thank Phillip Patton Ph.D., University of Nevada, Las Vegas, who provided valuable knowledge in the field of Diagnostic Health Physics and useful critiques and recommended changes throughout the paper. I would also like to thank Dr. David Steinberg and Dr Mark Winkler for allowing me the use of their CT units at Steinberg Diagnostic Imaging Centers, without whose assistance, this study would not have been possible.

I am also very appreciative to the entire CT department of Steinberg Diagnostic including but not limited to Lori Bieber R.T. (R) (CT), Chris Marshall R.T. (R) (CT), Tim Lehan R.T. (R) (CT), as well as Leonard Meyhew of Toshiba Service, whose technical abilities aided immensely in the completion of this study.

Finally, I thank my wife, Brenda, who has been most patient and gave me every encouragement when I needed it most.

CHAPTER 1

INTRODUCTION

1.1 History

Computed Tomography (CT) was the first medical imaging modality completely dependent on computer technology. The term tomography simply means picture (graph) of a slice (tomo). The first CT prototype, invented in the early 1970's by Sir Godfrey Hounsfield, was a dedicated head scanner capable of displaying the anatomy of the brain without over or underlying structures. This major advancement in diagnostic radiology, for which Hounsfield later earned a Nobel Prize, ushered in an era of high technology and non-invasive imaging. The Nobel Prize received by Hounsfield was shared with Allan MacLeod Cormack, a nuclear physicist at Tufts University, who helped conquer the mathematical problems associated with CT. The first whole-body CT scanner was developed in 1974 by Dr. Robert Ledley, a professor of radiology at Georgetown University. This new advancement by Ledley sparked the growth of CT, and the number of CT units installed worldwide increased dramatically.

The first CT scanner, or conventional scanner, provided one transaxial slice as the beam rotated 360 degrees around the patient. The beam would then be turned off, the table would be repositioned and another slice would be generated until the entire area of interest was covered. In spiral or helical scanners the beam is left on for the entire procedure while the table is continually advancing through the beam. This is much faster

than conventional scanners thus allowing for smaller slice thicknesses, which allows for an increase in resolution and a decrease in the possibility of overlooking a smaller lesion without increasing the total scan time. Multi-slice helical CT scanners image several slices simultaneously due to the multiple detectors present (currently up to 64 detector elements are used clinically). In practice, a multi-slice helical scanner acquires images two to three times faster than a single slice helical scanner.

There are presently seven generations of CT scanners with the term generation simply describing the method of scanning and does not necessarily infer an advancement in technology, but simply another approach to data acquisition (Seeram 2001). The seventh generation of CT scanners is the basis for this research project. The seventh generation is the newest and fastest of the modern CT scanners utilizing multiple detector banks with a helical or spiral pattern of acquisition used to generate multiple slices from a single x-ray beam. The helical acquisition pattern is generated from the movement of the imaging table through the x-ray beam while the beam is continuously rotating around the entire area of interest. This improvement in x-ray beam utilization allows for shorter scan times per patient; oftentimes the entire scan can be performed over the course of a single breath hold, which reduces artifacts generated by patient motion.

The rapid technological advances in CT over the past 30 years have resulted in a steady increase in the number of CT scans being performed annually, making it the major source of exposure to the population via diagnostic x-rays (Mettler et al. 2000). With this increased utilization, the concerns over patient radiation doses from CT have also grown (Mettler et al. 2000). Although CT studies only amount to about 5% of all X-ray examinations, it contributes approximately 40% of the collective dose to the population

from diagnostic radiology (Kwan et al 1998). This fact has made CT dosimetry an important topic in diagnostic radiology today. The introduction of multi-slice scanners has focused further attention on this issue, and it is generally believed multi slice scanners can lead to higher patient doses (Golding et al. 2002). This is due to the increased abilities and ease of use of the multi-slice scanners, i.e. increased volume coverage at higher tube currents with shorter scan times, which could lead to an increase in patient dose. This deviates from the standard assumption that under the same imaging parameters increased slice capabilities result in less dose. The overall goal of this paper is to investigate this hypothesis.

1.2 The Seven CT Generations

As mentioned previously the term generation does not necessarily imply advances in technology but this does not mean there have been no improvements as the generations have progressed but some generations are very similar in use to others but with varying geometry. First generation scanners utilized a pencil beam geometry which is defined by a set of parallel rays that generates a projection profile (Seeram 2001). These scanners were coined translate-rotate scanners because a highly collimated beam was used in conjunction with a detector to translate across the patient. Once across the patient, the tube and detectors then rotate one degree and translate across the patient as can be seen in Fig.1.1.

This would continue until 180 projections were acquired around the patient and thus was extremely time consuming; approximately four to five minutes to produce a complete scan. An advantage of first generation scanners was its efficiency of scatter

reduction. Since only one detector was used, any scatter that was deflected from the highly collimated beam was not measured by the detector. Even by today's standards first generation scanners offer the best scatter rejection.

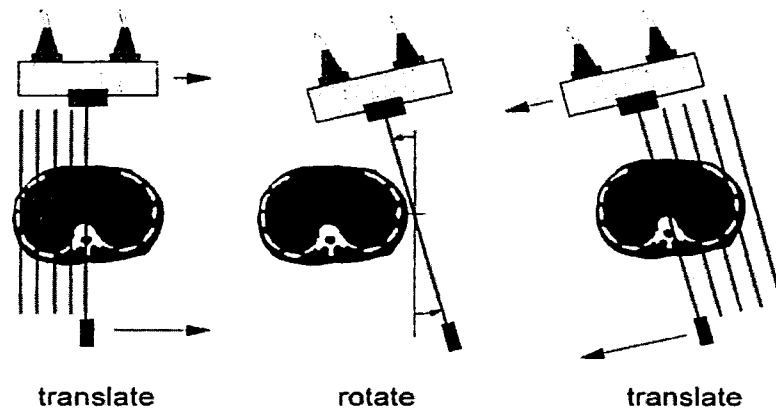


Figure 1.1. First generation (rotate/translate) computed tomography (CT). The x-ray tube and a single detector (per CT slice) translate across the field of view, producing a series of parallel rays. (Bushberg et. al. 2002).

Second generation scanners still utilized translate-rotate geometry but simply incorporated a fan beam and a greater number of detectors, usually thirty, which were placed in a linear array. This better utilized the x-ray beam and theoretically would reduce scan times by a factor of thirty. This was not the case however because the choice was made to increase the amount of data collected to increase image quality. However, the second generation models were still generally 15 times faster than the first generation models for comparable types of studies.

Third generation scanners implemented an even larger number of detectors, more than 800, and increased the angle of the beam which allowed total coverage of the patient without translation. A problem associated with this large number of detectors was the inability to keep the gain of each detector from drifting. This drift in gain led to artifacts

inherent to the third generation geometry known as ring artifacts. Ring artifacts are produced because every voxel within the object slice is not seen by every detector, therefore detector drift will only effect the voxels seen by that detector and is not averaged over all the voxels in that slice. An example of a third generation ring artifact is shown in Fig 1.2.

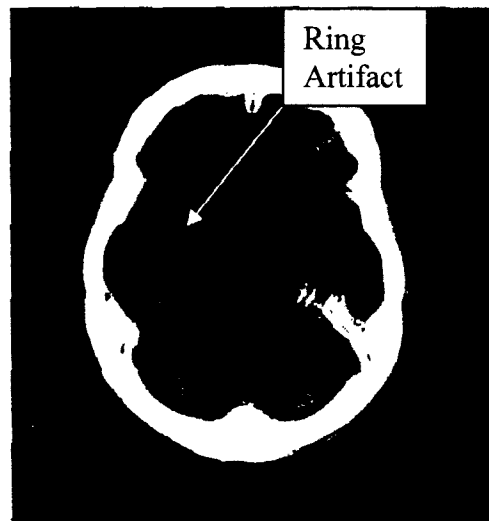


Figure 1.2. Clinical example of ring artifacts. (Morgan 1983).

These third generation scanners are known as rotate-rotate scanners referring to the rotation of the x-ray tube and the rotation of the detectors as shown in Fig.1.3.

With the elimination of the translate motion, scan times were reduced drastically to less than 5 seconds per slice (Bushberg et al. 2002). Third generation geometry first introduced in 1975 is still the most commonly used geometry for today's scanners and with the advances in calibration software, have become effectively free of ring artifacts (Bushberg et al. 2002).

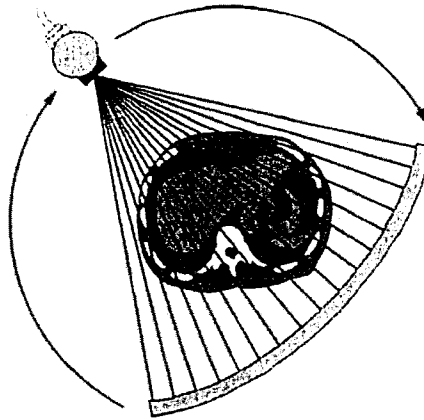


Figure 1.3. Third generation computed tomography. In this geometry, the x-ray tube and detector array are mechanically attached and rotate together inside the gantry. (Bushberg et al. 2002).

Fourth generation scanners were engineered to eliminate the ring artifacts associated with the third generation scanners. Fourth generation scanners implement a full ring, 360 degrees, of stationary detectors and a rotating beam thus termed a rotate-stationary geometry. These new scanners utilized approximately 4,800 individual detectors increasing the cost of the scanners. However, due to the fact that each detector acts as its own reference detector the dependence on uniform detector gains is eliminated and consequently so are the ring artifacts.

Fifth generation scanners are termed stationary-stationary because there are no moving parts associated with this scanner. It is targeted for cardiology uses and allows extremely fast scan times, on the order of 50 msec, which can generate fast-frame rate CT images of the beating heart (Bushberg et al. 2002).

Sixth generation scanners incorporated a new technological advancement known as a slip ring. In previous scanners the detectors and x-ray tube needed to be connected to the stationary electronic components of the scanner by wires. This meant that after each

360 degree, rotation the gantry would need to rotate 360 degrees in the opposite direction to keep the wire connections from being damaged. This was not time efficient because of dead times at the end of each rotation in which no data was being acquired. In the early 1990s the slip ring technology became available and allowed the gantry to rotate continuously without the tethers of wires connecting the detectors and tube to the electronic components of the scanner. The slip rings are electromechanical devices consisting of circular electrical conductive rings and brushes that transmit electrical energy across a rotating interface (Brunnett 1990). The ability to image continuously without the need to rewind cables or wires further decreased scan times. This slip ring technology allowed for a new type of acquisition termed helical scanning. Helical scanners allow data to be acquired continuously while the imaging table is being translated through the gantry. This constant movement of the x-ray tube and table produce a helical pattern around the patient as shown in Fig. 1.4.

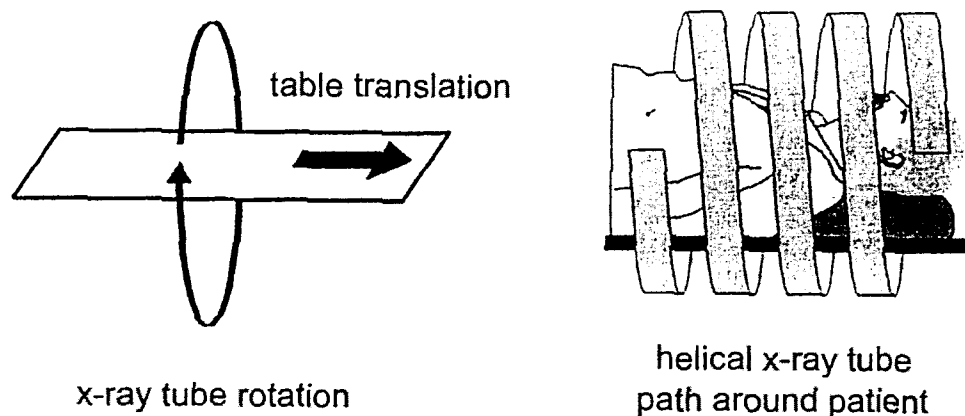


Figure 1.4. With helical CT scanners, the x-ray tube rotates around the patient while the patient and table are translated through the gantry. The net effect of these two motions results in the x ray tube traveling in a helical path around the patient (Bushberg et al. 2002).

Helical scanners reduce imaging times by avoiding the extra time associated with translating the patient table, and generally, an entire scan of the abdomen can be completed in approximately 30 seconds. Benefits of these shorter scan times include reduced artifacts due to patient motion as well as a reduction in the amount of contrast agent necessary to perform a study.

Seventh generation scanners, have overcome the physics that limit standard x-ray production due to tube overheating. This was accomplished by decreasing the amount of collimation and increasing the number of detectors in the z axis allowing for greater utilization of the x-ray beam and increased coverage. In older single array scanners, a decrease in the collimation of the beam would indeed allow for greater coverage and larger slice thickness, but would also decrease the spatial resolution in the slice thickness dimension. Multi-detector arrays allow slice thickness to be determined by the detector size and not by the beam collimation allowing for increased coverage with no loss in spatial resolution. The ability to increase coverage allows for a reduction in scan times, which is always beneficial in diagnostic imaging. The designs of single slice and multi-slice scanners are similar in most aspects that affect radiation dose, but multi-slice scanning can potentially result in higher radiation risk to the patient due to increased capabilities, which allow longer scan lengths at high tube currents (Lewis 2005). The newer multi-slice scanners better utilize the existing x-ray beam than did single slice scanners of the past. Single slice scanners were limited to lower mA and shorter scan lengths due to overheating of the tube. Multi-slice CT increased utilization of the existing beam allowing longer scan lengths at higher mA with less worry of tube overheating. These facts allow much more flexibility for the physician in generating scanning

protocols but with this increased flexibility comes the greater responsibility of safeguarding against unnecessary exposure.

1.3 Physics of Helical Scanning

The advent of helical scanners has brought forward many different considerations, both positive and negative in nature. An immediate problem was the fact that modern reconstruction algorithms for CT are based on the assumption that the x-ray source and detectors acquire data in an axial slice and not in the helical pattern that the newer CT scanners utilize. This is corrected by adding an interpolation phase to the processing of the raw data prior to the normal reconstruction utilized in conventional axial scanning. Interpolation is essentially a weighted average of the data from either side of the reconstruction plane, with slightly different weighting factors used from each projection angle (Bushberg et al. 2002). Although this does add another step to the processing of the acquired CT data it does afford a very important advantage. With standard axial scanning techniques, images are acquired contiguously and abut each other along the cranial-caudal axis of the patient. This is of importance due to the fact that the sensitivity of the CT image to objects not centered in the voxel is reduced (as quantified by the slice sensitivity profile), and therefore subtle lesions, which lie between two contiguous images may be missed (Bushberg et al. 2002). The major advantage of helical scanning is the ability to retrospectively reconstruct images at any position or interval in the volume area producing a scan that is almost uniformly sensitive to even subtle abnormalities that may have not been visualized by standard axial imaging due to its proximity to the edge of the voxel (Bushberg et al. 2002). A noted problem with helical scanners is the need for

additional information at each end of the planned image volume in order to provide enough information to interpolate the first and last images. This has been found to cause an increase in exposure outside of the imaged volume (Nicholson and Fetherston 2002). On single slice helical scanners an additional half or full rotation is generally required at each end of the imaged volume. For multi-slice helical scanners the number of extra rotations depends on a number of factors such as the interpolation method, the pitch and the reconstructed image width (Nicholson and Fetherston 2002). Each of these additional rotations can add substantially to the patient dose when compared to standard axial scanners. This can especially be true in smaller scan volumes, and in those cases, it may be preferable to perform the scan in the conventional slice by slice mode.

The term utilized in helical scanning to describe the table movement speed is pitch. Pitch is a ratio of the table movement per gantry rotation to the beam collimation. Values less than one alert the user that overscanning is occurring, causing unnecessary exposure to the patient and values greater than two alert the user that image quality may be degraded severely by underscanning. Pitches of 1.0 to 1.5 are commonly used with today's helical scanners, and manufacturers have spent a great deal of time, money, and effort to develop scan protocols which utilize this range of pitch (Bushberg et al. 2002). On multi-slice scanners the radiation dose is inversely proportional to pitch, if the tube current and tube potential are kept constant (i.e. the dose will be halved if the pitch is doubled) (Lewis 2005). With these factors in mind it is of utmost importance to understand the increased dose associated with multi-slice helical scanning and decreased pitches. If these points are fully understood, the advantages of decreased scan times,

increased sensitivity and a reduction in the amount of contrast needed are a compelling argument for their continued use.

1.4 Single Slice vs. Multi-slice CT

In previous generations of CT scanners only a single row of detectors were utilized, which limited the volume covered per 360° rotation of the x-ray beam, increasing scan times. The modern CT detectors are solid state in construction and are composed of a scintillator joined to a photodetector. The scintillator emits visible light which is captured by the photodetector when struck by x-rays (Seeram 2001). In single slice scanners, the detectors are about 15 mm, and the slice thickness is determined by collimators proximal to the beam origin (Bushberg et al. 2002). The slice width chosen for single slice scanners, varies widely depending on the organ or body part being imaged, but generally ranges from 1 mm to 10 mm. Increasing the slice width would limit the resolution capabilities of the scanner, therefore slice thicknesses are generally less than 3 mm. The multi-slice scanners have multiple rows of detectors varying in size from 0.5 mm to 5 mm. The advantages of multi-slice CT, as outlined by Saito (1998), include increased speed and volume coverage, improved spatial resolution and a more efficient use of the x-ray beam. It has been shown that a 4-slice helical CT scanner is approximately twice as fast as a single slice CT scanner while still allowing for a comparable image quality (Hu 1999). A comparison of the scanning times for 4-slice CT versus single slice CT can be seen in Table 1.1.

Table 1.1. Comparison of scanning times for a 4-slice CT and single-slice CT (Seeran 2001).

	SCAN AREA (mm)	SLICE THICKNESS (mm)	SCAN TIME(sec)	
			FOUR-SLICE	SINGLE-SLICE
Lung study	300	10	4	30
	300	3	15	100
Trauma case	1300	10	17	130
CT Angiography	40	1	5	40

Additionally the improved spatial resolution is due to the fact that multi-slice CT produces thin slices, approximately 1-2 mm, which allows for detection of smaller structures than the more commonly used wider slices of the single slice scanners (Seeram 2001). More efficient use of the x-ray beam is another benefit of multi-slice scanners. In a single slice scanner, the beam must be collimated down to dictate the slice thickness, whereas the beam is less collimated in the z direction for multi-slice scanners to allow for coverage of the entire array of detectors. With these above-mentioned advantages of multi-slice scanning, as compared to single slice, it is easy to see why the trend in most modern radiology departments is toward the purchase and utilization of multi-slice scanners.

1.5 CT Dosimetry

Exposure during a CT procedure is quite different than that received from conventional x-ray procedures, and specific dose calculation techniques have to be formulated in order to provide accurate assessment of patient dose. These dose calculations are utilized by the physician to weigh the risk verses benefits of ordering a CT scan for a particular patient. The radiation doses from CT scans, as mentioned

previously, are among the highest of all the diagnostic radiology procedures making it imperative to have an accurate determination of the patient's received dose. The primary interaction mechanism in CT is Compton scattering, so the dose attributed to scattered radiation is substantial and can even be higher than the dose from the primary beam (Bushberg et al. 2002). This scattered radiation is not confined within the collimated beam as the primary x-rays are, and therefore the acquisition of a CT slice delivers a considerable dose from scatter to adjacent tissues, outside the primary beam. In practical CT applications multiple contiguous slices are acquired over a specified volume resulting in slices receiving dose from the primary beam radiation as well as scattered radiation dose from the acquisitions of other slices that either abut it or are very close to it. There have been many different methods reported to calculate CT doses, but most are very time consuming and require highly specialized equipment. The easiest and most accurate method is the CT dose index (CTDI). In 1981 the Bureau of Radiological Health suggested an easy and accurate utilization of the CTDI and the multiple scan average dose (MSAD) to calculate patient dose (Seeram 2001). CTDI can be measured in any material and is given by the integral along a line parallel to the axis of rotation (z) of the dose profile, $D(z)$, for a single slice, divided by the nominal slice thickness (T) (Jessen et al. 1999), Equation 1:

$$CTDI = \frac{1}{T} \int_{-\infty}^{\infty} D(z) dz \quad (1)$$

These CTDI numbers are very useful for dose calculation of a single slice, but most CT examinations are composed of multiple slice scans; therefore, the MSAD has

been designed to cover these real world situations. For a sufficient number of slices such that the first and last slice do not contribute significant dose over the central slice, the MSAD is given by Equation 2 (Jessen et al. 1999):

$$MSAD = \frac{I}{T} CTDI \quad (2)$$

where T equals the slice thickness and I is the distance between successive slices. By utilizing the theory of volume averaging (Jucius and Kambic, 1977), a measurement with a standard 100 mm pencil shaped ionization chamber recorded for a single slice in a phantom is equivalent to a measurement at the midpoint of a series of contiguous slices covering the active length of the chamber (Ng et al. 1998). Based on this principle, MSAD can be easily measured and has become the recommended method of dose calculation by the American Association of Physicists in Medicine (AAPM) to be utilized for evaluation and acceptance testing of CT scanners. CTDI measurements are obtained by using a dosimeter with a 100 mm long pencil ionization chamber and a body or head CT polymethyl-methacrylate (PMMA) phantom.

CHAPTER 2

METHODS AND MATERIALS

2.1 Acquisition Systems

A dose comparison for different scanning protocols utilizing three different multi-slice helical CT scanners was performed. All three CT scanners being used are seventh generation helical Toshiba Aquillion®¹ scanners with 3rd generation geometries and varying slice capabilities of 4, 16, and 64 slices per 360 degree revolution. They have a wide area 2D detector design that utilizes present CT technology and can be operated in axial mode and helical scan mode to cover volumes beyond the detector's width. The technical specifications for the Toshiba Aquillion® CT scanners can be seen in Table 2.1.

Table 2.1. Technical specifications for the Toshiba Aquillion® CT scanners.

	4-SLICE	16-SLICE	64-SLICE
Number of detector elements	30464	35840	57344
Element sizes	1mm×1mm	1mm×1mm	1mm×1mm
Longitudinal FOV	4 mm	16 mm	32 mm
Data sampling rates	1800 views/sec	1800 views/sec	1800 views/sec
Dynamic range of analog to digital converter	18 bits	18 bits	18 bits

¹ Toshiba America, Inc. 1251 Avenue of the Americas, Suite 4110 New York, NY 10020

The detector elements consist of a scintillator attached to a photodiode, which are the predominant type of detectors in use in today's modern CT scanners. All three systems consist of three wedge designs (large, small, and flat). The large and small wedges are shaped to compensate for the variable path length of the patient across the scan FOV. The small wedge is used for an object under 240 mm FOV (e.g. head and pediatric patients), and the large wedge is used for over 240 mm FOV (e.g. chest and abdomen scans). The flat wedge is thicker at the center than the other wedges. A Feldkamp-Davis-Kress (FDK) algorithm (Feldkamp et al. 1984) is used for reconstruction. All other data processing and interpretation is performed with a high-speed image processor with field programmable gate-array based (FPGA) architecture. It takes less than 1 sec to reconstruct volume data of a $512 \times 512 \times 256$ matrix.

2.2 Phantoms

Standardized CTDI head and abdomen phantoms (76-414-4150 Nuclear Associates)² composed of polymethyl-methacrylate (PMMA) were used in all dose measurements. The CTDI phantoms, were designed in accordance with the Food and Drug Administrations performance standards specifically applicable to CT systems as described in 21 CFR 1020.33 (Cardinal Health, 1991). By definition, a CTDI phantom is a phantom used for the determination of the dose delivered by a CT x-ray system, and shall be a right circular cylinder of PMMA with a density of 1.19 ± 0.01 grams per cubic centimeter (Cardinal Health, 1991). The phantom shall be at least 14.0 cm in length and have diameters of 32.0 cm for testing any CT system designed to image any section of the body (whole body scanners) and 16.0 cm for any system designed to image the head

² Fluke Biomedical, Nuclear Associates. 6045 Cochran Road. Cleveland, OH 44139

(head scanners) or for any whole body scanner operating in the head scanning mode. The phantom must allow means for the placement of a dosimeter along its axis of rotation and along a line parallel to the axis of rotation 1.0 cm from the outer surface and at the center of the phantom (21 CFR 1020.33, 2003). The CTDI phantoms used in this study, as seen in Fig. 2.1, have a diameter of 160 mm for the head and 320 mm for the abdomen with both having a length of 150 mm and five probe holes; one in the center and four around the perimeter, 90 degrees apart and 1 cm from the edge. These conventional phantoms contain holes just large enough to accept the pencil-shaped ionization chamber utilized for this study. Each phantom includes five acrylic rods for filling the holes in the phantom when not occupied by the dosimeter.

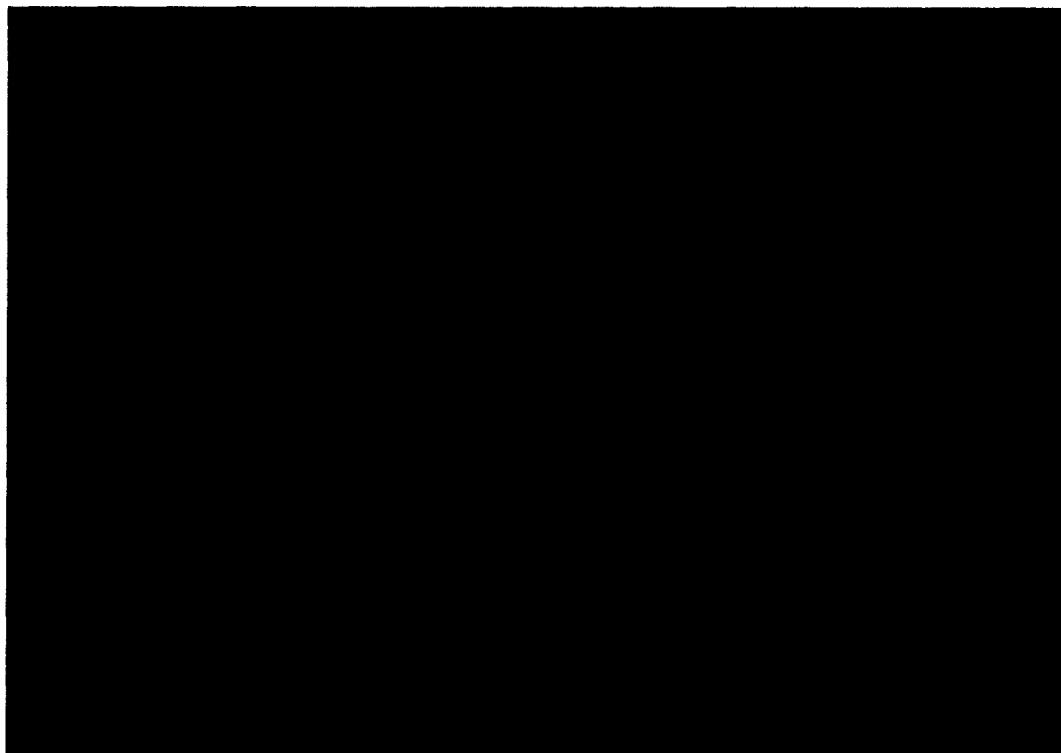


Figure 2.1. Standard CTDI head and abdomen phantoms.

2.3 Detector

A pencil-shaped ionization chamber (10X9-3CT Radcal®)³ of active length 100 mm was connected to a dosimeter (9095 Radcal®) and used to perform dose measurements. The ionization chamber is composed of C552 air equivalent walls and a polyacetal exterior cap with a 3 cm³ active volume. The minimum rate of detectable exposure is 20 nGy/sec with a maximum exposure rate of 350 mGy/sec. The maximum dose that can be accurately recorded is 1.4 kGy. The dosimeter was calibrated by Radcal Corporation for the appropriate radiation qualities on April 14, 2006.

2.4 Scanning Techniques

This study consists of a simple repeated measurement design and was performed at Steinberg Diagnostic Medical Imaging Centers (SDMI) of Las Vegas, Nevada. Scans were performed utilizing the afore mentioned CTDI head and abdomen phantoms in both axial and helical modes. The axial scans were acquired in a service mode of operation due to the fact that in normal scanning mode, Toshiba's multi-slice scanners default to a four-slice scanner when operated in axial mode. If service mode was not utilized these scans would simply be a comparison of three different four-slice CT scanners. Operating in service mode allows the nominal beam width to be expanded to encompass the full area of the detectors, i.e. 4 mm's for the four-slice, 16 mm's for the sixteen-slice and 32 mm's for the sixty four-slice. The axial scans were performed in a step and shoot manner beginning on the probe end of the CTDI phantom. The scanner performs one rotation around the phantom and then is manually moved 4 mm, 16 mm or 32 mm, depending on the particular scanner, and sequential scans were performed until the entire 96 mm of the

³ Radcal Corporation, 426 West Duarte Road, Monrovia, CA 91016

scanned volume was covered. Two sets of helical acquisitions were acquired in normal scanning mode with the head and body phantoms. The main differences between the two helical acquisitions was the distance scanned and the mA used. Pitch factors were difficult to keep constant in helical mode due to variations in the slice capabilities of the scanners but the variations were kept to a minimum. Dosimetry measurements were made in all four outer probe holes and four measurements were taken in the center probe hole. The phantom was placed in the center of the scanner's aperture for the six protocols mentioned. The acquisition parameters for the helical scans can be seen in Tables 2.2, 2.3, and 2.4, and the axial scan parameters can be seen in Tables 2.5, 2.6, and 2.7.

Table 2.2. Parameters for 4-slice Toshiba Aquillion® CT scanner helical acquisitions.

	Head Helical Set 1	Head Helical Set 2	Abdomen Helical Set 1	Abdomen Helical Set 2
kVp	120	120	120	120
mA	300	200	300	200
Time per revolution (sec)	1	1	0.5	0.5
FOV	240 mm	240 mm	400 mm	400 mm
Range	154 mm	96 mm	154 mm	98 mm
Pitch	0.88	0.88	0.88	0.88
Nominal beam width	4.0 mm	4.0 mm	4.0 mm	4.0 mm

Table 2.3. Parameters for 16-slice Toshiba Aquillion® CT scanner helical acquisitions.

	Head Helical Set 1	Head Helical Set 2	Abdomen Helical Set 1	Abdomen Helical Set 2
kVp	120	120	120	120
mA	300	200	300	200
Time per revolution (sec)	1	1	0.5	0.5
FOV	240 mm	240 mm	400 mm	400 mm
Range	154 mm	96 mm	154 mm	98 mm
Pitch	0.94	0.94	0.94	0.94
Nominal beam width	16.0 mm	16.0 mm	16.0 mm	16.0 mm

Table 2.4. Parameters for 64-slice Toshiba Aquillion® CT scanner helical acquisition.

	Head Helical Set 1	Head Helical Set 2	Abdomen Helical Set 1	Abdomen Helical Set 2
kVp	120	120	120	120
mA	300	200	300	200
Time per revolution (sec)	1	1	0.5	0.5
FOV	240 mm	240 mm	400 mm	400 mm
Range	155 mm	100 mm	154 mm	98 mm
Pitch	0.91	0.91	0.91	0.91
Nominal beam width	32.0 mm	32.0 mm	32.0 mm	32.0 mm

Table 2.5. Parameters for 4 slice Toshiba Aquillion® CT scanner axial acquisitions.

	Head Axial	Abdomen Axial
kVp	120	120
mA	200	200
Time per revolution (sec)	1	1
FOV	240	400
Range	96	96
Nominal beam width	4 mm	4 mm

Table 2.6. Parameters for 16 slice Toshiba Aquillion® CT scanner axial acquisitions.

	Head Axial	Abdomen Axial
kVp	120	120
mA	200	200
Time per revolution (sec)	1	1
FOV	240	400
Range	96	96
Nominal beam width	16 mm	16 mm

Table 2.7. Parameters for 64 slice Toshiba Aquillion® CT scanner axial acquisitions.

	Head Axial	Abdomen Axial
kVp	120	120
mA	200	200
Time per revolution (sec)	1	1
FOV	240	400
Range	96	96
Nominal beam width	32 mm	32 mm

Since the pitch varied slightly it was important to look at the effect of pitch on dose. As mentioned previously if the tube current and potential are kept constant and the pitch is doubled the dose will be halved. To validate this statement we performed four center cavity measurements utilizing the helical head set 2 protocol with three different pitches on each scanner. With the above mentioned information regarding the theoretical relationship between dose and pitch the point was to select minimum and maximum pitch values where one would be half of the other, therefore the two chosen for all three scanners was 0.7 and 1.4. The third pitch value varied slightly for each of the scanners, 0.88, 0.94 and 0.91, for the 4-slice, 16-slice and 64-slice scanners, respectively.

2.5 Dose Measurements

The dose from all scans on the three CT scanners was measured with the 100 mm long pencil shaped ionization chamber placed in the phantom's various cavities while scanning ≈ 154 mm of the phantom's length, in set 1 of the helical acquisitions, and ≈ 96 mm of the phantom's length for all other acquisitions. The head phantom was placed in the CT scanners head holder with the foam pad removed, and its center was aligned at the isocenter of the CT scanner with the four outer cavities placed at the 12, 3, 6, and 9 o'clock positions. The abdomen phantom was placed directly on the patient table and positioned exactly the same as the head phantom. The ionization chamber was inserted sequentially into the central cavity and the four peripheral cavities of the phantom (other cavities not being used were filled with PMMA rods). Four exposures were measured for the central cavity followed by one measurement in each of the outer cavities. This procedure was repeated for all six of the scanning protocols utilized in this study. The scans to assess pitch effects were performed with the head phantom positioned as mentioned above and four central cavity measurements were taken. No outer cavity measurements were taken for the pitch assessment.

2.6 Dose Assessment

The dose was assessed using the CTDI_{vol} over varying scan lengths, (96 mm to 155 mm) as shown in Tables 2.2 – 2.7. CTDI_{vol} is a measure of exposure per slice and is independent of scan length. The CTDI_{vol} for a given scan series can be calculated by applying weighting factors to measurements given by the output of the pencil ionization chamber at both the center and periphery of the CTDI phantom. This weighted average

also takes into account the pitch factor when calculating dose received during helical studies. The $CTDI_{vol}$ is given by Equation 3:

$$CTDI_{vol} = \frac{1/3CTDI_{100(center)} + 2/3CTDI_{100(periphery)}}{p} \quad (3)$$

Where the $CTDI_{100(center)}$ is calculated from measurements with the probe in the central cavity of phantom, $CTDI_{100(periphery)}$ is calculated from measurements with the probe in the outer cavities and p is the pitch used during the scans. The $CTDI_{100}$ values are calculated from Equation 4.

$$CTDI_{100} = \frac{(L * C * f * E)}{(N * T)/100} \quad (4)$$

where:

- L = Active length of pencil ion chamber
- C = Calibration factor for electrometer
- f = 0.87
- E = Average measured exposure in mR
- N = Actual number of data channels used during one axial acquisition
- T = Nominal slice width of one axial image

The four central cavity measurements for each protocol were averaged to produce the $CTDI_{100(center)}$ for each specific protocol. The same was also done for the outer measurements to produce the $CTDI_{100(periphery)}$. Another term used to express CT dose that is being utilized by several manufacturers is the dose length product (DLP). The DLP will also be determined for the data and is simply the product of the $CTDI_{vol}$ and the length of each particular scan, The DLP is calculated from Equation 5:

$$DLP = CTDI_{vol} \times L \quad (5)$$

where L is the length of the area being scanned.

There are numerous CTDI spreadsheets being utilized in the field of dosimetry today, and they all are based on the acquisition of axial scans and are designed to estimate helical scan dose based on this data. An example of the spreadsheet utilized in this study can be seen in Fig 2.2.

As can be seen in Fig. 2.2, the kVp, mA, time per rotation, z-axis collimation (slice thickness) and scan length are accounted for when generating dose values. The axial scan exposure data is entered, both central and peripheral exposure measurements, into the spreadsheet where a weighted $CTDI_w$ value is calculated. This $CTDI_w$ value is the dose if the scan was acquired in axial mode, but to generate a helical scan dose the $CTDI_w$ must be divided by the pitch to account for the table translation during acquisition, to produce the $CTDI_{vol}$ dose. The complete set of CTDI calculation sheets can be viewed in Appendix A. There is a concern that there may be an underestimation of dose utilizing this technique. This is due to the previously mentioned extra revolutions of the scanner needed outside of the volume of interest for interpolation of the first and last slices of the scan (Nicholson and Fetherston 2002). The dose from these extra revolutions is not taken into account when only axial acquisition data is used to generate dose values for helical scans. A comparison of the axial head and helical head set 2 data is being performed to determine if there is in fact any underestimation of the dose received during a helical acquisition, if exposures are not acquired utilizing helical protocols. These CTDI calculation sheets can be viewed in Appendix B.

CT Equipment Information

DEP Facility Number:			SDMI	
Type:	Axial	x	Toshiba	
	Helical		CT Manufacturer	
	Total No. of Detectors	4	Jim Kelley	
			Physicist's Name and Date Performed	

Ionization Chamber Instrumentation

Manufacturer and Model	Radcal 9095		
Last Date of Calibration	4/14/2006		
Active Chamber Length (L) (mm)	100		
Chamber Correction Factor (C)	1		

Patient Scan Protocol

Procedure Type:	Head	
kVp	120	Procedures Types Not Performed by Facility
mA	200	
Exposure time per rotation	1	
Z axis collimation (T) (mm)	1.00	
# of data channels used (N)	96	
If Axial: Table Increment (I)(mm) OR If Helical: Table Speed (I) (mm/rot)	96.00	

Scan Measurements

At Isocenter of Phantom		
1st Measurement (mR)*	5849.0	
2nd Measurement (mR)*	5849.0	
3rd Measurement (mR)*	5849.0	
Average Measurement (mR)	5849.0	CTDI _{iso} (mR) 53.01
At 12 o'clock Position of Phantom		
		* Measurements must be w/i 5% of each other
1st Measurement (mR)*	6692.0	
2nd Measurement (mR)*	6692.0	
3rd Measurement (mR)*	6692.0	
Average Measurement (mR)	6692.0	CTDI _{max} (mR) 60.65

CT Dose Calculations and Pitch

CTDI _w (mGy)	58.10	CTDI _{vol} (mGy)	58.10
Pitch	1.000		

Figure 2.2. Standard CTDI dose calculation sheet as used for the 4-slice axial head scans.

The effective dose, in Sieverts (Sv), will be determined based on the DLP values calculated for each individual scan. The effective dose is the “sum over specified tissues of the products of the equivalent dose in a tissue and the weighting factor for that tissue” (Hall 2000). The effective dose takes into account that different types of radiations are more damaging than others, and that different body tissues are more radiosensitive than others. This allows for a more accurate determination of the biological effect of the procedure. The American College of Radiology (ACR) has adopted a simple conversion process for CT, dependent on what body part is being scanned (head or abdomen), where the effective dose is the product of the DLP times a constant, 0.0023 for the head and 0.015 for the abdomen.

CHAPTER 3

RESULTS

3.1 Axial Exposure Measurements

The axial exposure measurements for all three CT scanners are summarized in Tables 3.1, 3.2, and 3.3. Tables 3.1 - 3.3 show that the axial values are consistent for repeated scans at the central locations, with standard deviations ranging from 3.4 to 18.6 mR for each type of scan and for each scanner. The peripheral measurements displayed a little more fluctuation, with standard deviations ranging from 118 to 304 mR, for each type of scan and for each scanner. When comparing the head axial (HA) scans to the abdominal axial (AA) scans for each scanner, there was a decrease in exposure measurements in the abdomen scans in relation to the head scans. This is a direct effect of the field of view (FOV) size. The head protocols employed a 240 mm FOV while the abdomen protocols employed a 400 mm FOV. Utilizing a smaller FOV focuses the x-ray beam into a smaller area increasing the photon density. This increased photon density increases the exposure measurements; conversely, the larger FOV disperses the x-ray beam, decreasing the photon density and ultimately decreasing the exposure measurements. The average decrease, in central cavity measurements, from the HA scans to the AA scans was 64% (5089 mR vs. 1815 mR), 65% (3571 mR vs. 1243 mR) and 67% (3323 mR vs. 1090 mR) for the 4, 16 and 64-slice scanners, respectively.

Table 3.1. Axial exposure measurements and averages, in mR, for the 4-slice Toshiba Aquillion® CT scanner, with standard deviations in parenthesis.

4-Slice	Center (mR)	Peripheral				Average
		12 o'clock	3 o'clock	6 o'clock	9 o'clock	
Head	5099	5985	5703	5800	5800	5822 (118)
	5090					
	5085					
	5083					
Average	5089 (7.1)					
Abdomen	1819	4028	3778	3450	4054	3828 (281)
	1815					
	1811					
	1813					
Average	1815 (3.4)					

Table 3.2. Axial exposure measurements and averages, in mR, for the 16-slice Toshiba Aquillion® CT scanner , with standard deviations in parenthesis.

16-Slice	Center (mR)	Peripheral				Average
		12 o'clock	3 o'clock	6 o'clock	9 o'clock	
Head	3572	4306	4070	3911	3787	4069 (171)
	3574					
	3569					
	3569					
Average	3571 (3.9)					
Abdomen	1216	3125	3011	2445	2985	2892 (304)
	1257					
	1247					
	1253					
Average	1243 (18.6)					

Table 3.3. Axial exposure measurements and averages, in mR, for the 64-slice Toshiba Aquillion® CT scanner, with standard deviations in parenthesis.

64-Slice	Center (mR)	Peripheral				Average
		12 o'clock	3 o'clock	6 o'clock	9 o'clock	
Head	3318	4057	3897	3722	3717	3848 (162)
	3333					
	3321					
	3320					
Average	3323 (6.8)					
Abdomen	1100	3110	2809	2734	3054	2927 (183)
	1087					
	1082					
	1091					
Average	1090 (7.6)					

The exposure measurements of the 4-slice scanner, it can be noted that all were higher than the comparable protocols for the 16 and 64 slice scanners. The percent decrease, in central cavity measurements, of the 16-slice relative to the 4-slice for the HA and AA scans was 30% (5089 mR vs. 3571 mR) and 32% (1815 mR vs. 1243 mR), respectively. The percent decrease, in central cavity measurements, of the 64-slice relative to the 4-slice for the HA and AA scans was 35% (5089 mR vs. 3323 mR) and 40% (1815 mR vs. 1090 mR), respectively. Additionally the average peripheral measurements for the HA and AA were 14% (5089 mR vs. 5822 mR) and 111% (1815 mR vs. 3828 mR) higher than the average central measurements for the 4-slice scanner. This large variation is due to two reasons. Firstly, the head phantom is 16 cm in diameter and the abdomen phantom is 32 cm in diameter, which means that the abdomen phantoms surface is 8 cm closer to the x-ray source than the head phantom. The second factor being that the x-ray beam must travel through an extra 8 cm of PMMA in the

abdomen phantom in order to be measured in the central cavity leading to increased attenuation of the x-ray beam.

When reviewing the 16-slice exposure measurements, it can be noted that all were higher than the comparable protocols for the 64-slice scanner. The percent decrease, in central cavity measurements, upon comparison of the 64-slice to the 16-slice for the HA and AA scans was 7% (3571 mR vs. 3323 mR) and 12% (1243 mR vs. 1090 mR) respectively. The average peripheral measurements for the HA and AA were 14% (3571 mR vs. 4069 mR) and 132% (1243 mR vs. 2892 mR), higher than the average central measurements.

3.2 Helical Exposure Measurements

The helical exposure measurements for all three CT scanners are summarized in Tables 3.4, 3.5, and 3.6. Tables 3.4 - 3.6 show that the values also are consistent between repeated scans for the central measurements, with standard deviations ranging from 2.1 to 28.9 mR for each type of scan and for each scanner. The peripheral measurements displayed slightly more fluctuation, with standard deviations ranging from 36 to 210 mR. The exposure values for the helical head set one (HH1) were higher than the exposure values for helical head set two (HH2) on all scanners because of two factors. The first being HH1 was scanned at a higher tube current, 300 mA, as apposed to the HH2 scans 200 mA, and the range for HH1 was longer, 154 mm, as apposed to 98 mm for the HH2 scans. The increase in mA directly increases the number of photons delivered to the target, therefore, increasing the exposure. The increase in range also increases the exposure because the exposure time is increased. This same relationship was seen

between the helical abdomen set one (HA1) and the helical abdomen set two (HA2) exposures as well.

Table 3.4. Helical exposure measurements and averages, in mR, for the 4-slice Toshiba Aquillion® CT scanner, with standard deviations in parenthesis.

4-Slice	Center (mR)	Peripheral				Average
		12 o'clock	3 o'clock	6 o'clock	9 o'clock	
Head	10330	11620	11150	11230	11430	11358 (210)
Helical	10340					
Set 1	10300					
	10370					
Average	10335 (28.9)					
Head	6351	7370	6955	6998	7090	7103 (186)
Helical	6345					
Set 2	6344					
	6355					
Average	6349 (5.2)					
Abdomen	2019	3937	3748	3892	3863	3860 (102)
Helical	2012					
Set 1	2023					
	2015					
Average	2017 (4.8)					
Abdomen	1113	2398	2316	2082	2310	2277 (135)
Helical	1110					
Set 2	1110					
	1108					
Average	1110 (2.1)					

Table 3.5. Helical exposure measurements and averages, in mR, for the 16-slice Toshiba® Aquillion CT scanner, with standard deviation in parenthesis.

16-Slice	Center (mR)	Peripheral				Average
		12 o'clock	3 o'clock	6 o'clock	9 o'clock	
Head	6816	7310	7287	7213	7223	7258 (48)
Helical	6785					
Set 1	6776					
	6775					
Average	6788 (19.2)					
Head	4244	4852	4605	4477	4627	4640 (156)
Helical	4241					
Set 2	4232					
	4234					
Average	4238 (5.7)					
Abdomen	1344	2319	2314	2088	2367	2272 (125)
Helical	1352					
Set 1	1343					
	1341					
Average	1345 (4.8)					
Abdomen	816	1513	1561	1286	1430	1448 (121)
Helical	800					
Set 2	801					
	799					
Average	804 (8.0)					

Table 3.6. Helical exposure measurements and averages, in mR, for the 64-slice Toshiba® Aquillion CT scanner, with standard deviation in parenthesis.

64-Slice	Center (mR)	Peripheral				Average
		12 o'clock	3 o'clock	6 o'clock	9 o'clock	
Head	7504	8460	8153	8104	8020	8184 (192)
Helical	7494					
Set 1	7501					
	7511					
Average	7503 (7.0)					
Head	4799	5316	5098	5024	5079	5129 (128)
Helical	4785					
Set 2	4813					
	4817					
Average	4804 (14.5)					
Abdomen	1650	2875	2874	2818	2903	2868 (36)
Helical	1637					
Set 1	1647					
	1644					
Average	1644 (5.6)					
Abdomen	1041	1872	1849	1816	1900	1859 (36)
Helical	1016					
Set 2	1025					
	1040					
Average	1031 (12.1)					

The percent decrease in dose was consistent when comparing, central cavity measurements, of the HH1 to HH2 and the AH1 to AH2 for each scanner. For the 4-slice the decrease from HH1 to HH2 was 39% (10335 mR vs. 6349 mR) and the corresponding decrease for AH1 to AH2 was 44% (2017 mR vs. 1110 mR). For the 16-slice the decrease from HH1 to HH2 was 38% (6788 mR vs. 4238 mR) while the decrease from AH1 to AH2 was 40% (1345 mR vs. 804 mR). For the 64-slice the decrease from HH1 to HH2 was 36% (7503 mR vs. 4804 mR) and for the AH1 to the AH2 was 37% (1644 mR vs. 1031 mR). When comparing the helical head scans to the helical abdomen scans on all scanners, there was a decrease in exposure measurements of the abdomen scans in relation to the head scans. This decrease is a direct effect of the FOV size, as previously explained in the axial exposure measurements section, and the scan time. The scan times were shortened by decreasing the time per revolution from 1.0 sec, for the helical head scans, to 0.5 sec for the helical abdomen scans. This shortening of the exposure time reduces the number of photons incident on the phantom contributing to the decrease in the measured values.

For the 4-slice helical scanner, as seen in Table 3.4, it can be noted that all exposures were higher than the comparable protocols for the 16 and 64 slice scanners. On average, the reduction in central cavity measurements for all protocols was 32% when comparing the 16-slice to the 4-slice scanner and 19% when comparing the 64-slice to the 4-slice. The reduction in central cavity exposures for the head protocols on the 16 and 64-slice scanners compared to the 4-slice were more consistent than the abdomen protocols. The 16-slice HH1 and HH2 protocols decreased by 34% (10335 mR vs. 6788 mR) and 33% (6349 mR vs. 4238 mR), respectively while the 64-slice HH1 and HH2 protocols

decreased by 27% (10335 mR vs. 7503 mR) and 24% (6349 mR vs. 4804 mR), respectively. The 16-slice AH1 and AH2 protocols were reduced by 33% (2017 mR vs. 1345 mR) and 28% (1110 mR vs. 804 mR) while the 64-slice AH1 and AH2 were reduced by 18% (2017 mR vs 1644 mR) and 7% (1110 mR vs. 1031 mR), respectively.

When analyzing the 16-slice helical data, in Table 3.5, the exposure measurements were less than those of the 64-slice, ranging from 10-22%, for all of the helical protocols. The average decrease, in central cavity measurements, was 16% for all helical scans, from the 64-slice to the 16-slice scanner. This finding was of significance because the standard belief regarding multi-slice helical scanners is that increasing the slice capabilities of the scanners would decrease the associated dose if all other factors remained constant. The findings here seem to directly disagree with that standard assumption. The reduction in exposure measurements when comparing the average central to average peripheral measurements of the HH1, HH2, AH1, and AH2 were 6%, 9%, 41% and 44%, respectively. As mentioned previously these large differences in central to peripheral measurements between the head and abdomen scans can be accounted for by the decreased distance of the phantom to the x-ray source in the case of the abdomen phantom and is compounded by the increased amount of PMMA that the beam must travel through in comparison to the head phantom.

3.3 CTDI_{vol} Results

To simply use exposure values for dose assessment would limit the ability to account for variations in scanning techniques such as pitch, range and variations in electrometers. To account for these factors the standard method of dose calculation

utilizes the computed tomography dose index (CTDI). The CTDI values for both the central and peripheral exposures are calculated using Eq. 4 of Section 2.6. A weighting factor is then applied to the central and peripheral CTDI values as well as a pitch correction, if a helical scan was performed, to calculate the $CTDI_{vol}$ as seen in Eq. 3, also in Section 2.6. Table 3.7 compares the calculated CTDI values to the measured exposure values for the 4-slice scanner.

Table 3.7. Calculated $CTDI_{vol}$ values, in mGy, for the 4-slice Toshiba Aquillion CT scanner utilizing recorded exposure values compared to CTDI values.

	Exposure Values (mGy)	CTDI values (mGy)
HA	55.22	58.1
HH1	123.94	81.01
HH2	77.08	79.67
AA	31.25	32.89
AH1	36.51	24.05
AH2	21.24	21.96

Utilizing the recorded exposure values instead of the calculated CTDI values produced underestimations of dose for the HA, HH2, AA, and AH2 scans of 5%, 3%, 5% and 1% respectively. The HH1 and AH1 scans however, were overestimated by 53% and 52% respectively. The large overestimations were both on scans that were 154 mm in length while the four underestimated scans were only 94 mm in length. This would suggest that the CTDI values become increasingly important at longer scan lengths, which is more consistent with patient scan lengths. This would be expected after reviewing Eq. 4 of Section 2.6. Equation 4 divides out the product of the number of data channels used and the nominal slice width, i.e. the range of the scan, to produce a per slice dose that can be more easily applied to a scan of any other length, where as the

exposure is highly dependent on the length of the scan. The actual calculated CTDI_{vol} values for all the scans performed in this study can be seen in Table 3.8.

Table 3.8. CTDI_{vol} values in mGy for the 4, 16, and 64-slice Toshiba Aquillion® CT scanners, with standard deviation in parenthesis.

	4-Slice (mGy)	16-Slice (mGy)	64-Slice (mGy)
Axial Head	58.10 (1.18)	40.66 (1.71)	38.26 (1.62)
Helical Head Set 1	81.01 (2.12)	49.31 (0.52)	56.43 (1.92)
Helical Head Set 2	79.67 (1.86)	48.98 (1.56)	55.17 (1.29)
Axial Abdomen	32.89 (2.81)	24.40 (3.05)	24.11 (1.83)
Helical Abdomen Set 1	24.05 (1.02)	13.63 (1.25)	17.58 (0.36)
Helical Abdomen Set 2	21.96 (1.35)	13.41 (1.21)	17.79 (0.38)

The calculated values for the CTDI_{vol} showed a definitive drop in dose for all protocols when comparing the 16-slice and 64-slice CT to that of the 4-slice CT. This was not the case, however when comparing the 64-slice to the 16-slice. The 64-slice dose exhibited a slight increase in dose when compared to the 16-slice for all of the helical scans performed, while the axial scans did continue to follow the pattern of reduced dose. The percent decrease in dose from the 4-slice to the 16-slice for the AH, HH1, HH2, AA, AH1, and AH2 was 30%, 39%, 39%, 26%, 43% and 39%, respectively. The percent decrease in dose from the 4-slice to the 64-slice for the AH, HH1, HH2, AA, AH1, and AH2 was 34%, 30%, 31%, 27%, 27% and 19%, respectively. The percent decrease in

dose from the 16-slice to the 64-slice for HA and AA was 6% and 1%, respectively. Where as the percent increase for the HH1, HH2, AH1 and AH2 was 14%, 13%, 29% and 33%, respectively. The CTDI calculation sheets can be reviewed in Appendix A.

3.4 DLP Results

The dose length product (DLP) is a practical quantity that expresses the total energy deposited by x-rays over the entire length of the scan. The $CTDI_{vol}$ is an expression of dose for a slice but the DLP provides a summation of dose for all the slices, and thus the DLP is the product of the $CTDI_{vol}$ and the scan length. Most manufactures are now displaying both the DLP and $CTDI_{vol}$ values on the scanner monitor. For this study, the DLP values were calculated for each scanner and protocol and can be seen in Table 3.9.

Table 3.9. DLP values, in mGy-cm, for the 4, 16, and 64-slice Toshiba Aquillion® CT scanners.

Scan	(mGy cm)	4-Slice	16-Slice	64-Slice
Axial Head		557.8	390.3	367.3
Helical Head Set 1		1247.6	759.4	874.7
Helical Head Set 2		780.8	480.0	551.7
Axial Abdomen		315.7	234.2	231.5
Helical Abdomen Set 1		370.4	209.9	270.7
Helical Abdomen Set 2		215.2	131.4	174.3

The DLP values give a better representation of the dose received from the performed scans, due to the fact that it takes into account the entire scanned length. The HH1 had the highest DLP value of any of the helical scans, which would be expected due to the length of the scan being 154 mm as apposed to 96 mm for the rest of the helical scans performed. Likewise the AH scan had the highest DLP of the axial scans. Upon review of the data it can be noted that the DLP values for the 4-slice were all higher than the comparable protocols for the 16 and 64 slice scanners. The axial scan DLP's continued to decrease from the 16-slice to the 64-slice protocols but as seen with the previous helical scan data the helical DLP's increased from the 16-slice scans to the 64-slice scans.

3.5 CT Dose Relationship to Pitch

Three varying pitch factors were applied to the HH2 protocol utilizing the minimum and maximum pitches available for the CT scanners that would allow one pitch to be 50% of the other. This was performed to test that if the tube current and potential are kept constant and the pitch is doubled, the dose will be halved. The measurements recorded with the varying pitch factors for all three scanners are summarized in Table 3.10.

There is a positive result for dose being reduced by a factor of one-half when the pitch was doubled. All values measured at the 1.4 pitch value were $\approx 50\%$ of the measurements made at the 0.7 pitch. This verifies that doubling the pitch reduces the exposure by one-half.

Table 3.10. Exposure measurements at center of phantom, in mR, of varying pitch factors for the 4, 16, and 64-slice Toshiba Aquillion® CT scanners.

	Pitch Factors		
	0.7	0.9	1.4
4-Slice (mR)	7888	6351	3949
	7897	6345	3952
	7873	6344	3955
	7891	6355	3950
16-Slice (mR)	5658	4244	2844
	5656	4241	2841
	5668	4232	2840
	5671	4234	2840
64-Slice (mR)	6207	4799	3124
	6224	4785	3123
	6211	4813	3119
	6220	4817	3121

3.6 Helical Dose Estimation

The comparison of dose calculation for helical scans utilizing helical scan exposures to a calculated dose of helical scans utilizing axial exposures, as suggested by the ACR, was performed and is summarized in Table 3.11. The CTDI calculation sheets can be seen in Appendix B. The ACR helical doses were calculated from the AH scans of each CT scanner. The helical dose values were calculated from the HH2 of each of the CT scanners. These two sets of data were chosen because they were identical in all acquisition parameters except that one was acquired in helical mode while the other was acquired in axial mode.

Table 3.11. Comparison of CTDI_{vol} dose values, in mGy, calculated from exposures acquired from axial scans and true helical scans.

	ACR Calculated Helical Dose (mGy)	Actual Helical Dose (mGy)	Percent Difference
4-Slice	66.21	79.67	16.9
16-Slice	43.32	48.98	11.6
64-Slice	42.03	55.17	23.8

There was a sizable underestimation of dose when utilizing axial exposures to calculate helical dose, with the largest underestimation, of 23.8% coming from the 64-slice scanner. This does seem to support the argument that the dose received by the extra revolutions outside of the imaged volume from helical scanning necessary for interpolation of the first and last slice is ignored when utilizing axial exposure data. Even though the pitch factor is accounted for, there is still quite a large underestimation of dose. This would suggest that when it is necessary to calculate helical CTDI, the scans must be acquired in helical mode to provide accurate results.

3.7 Effective Dose Results

The effective dose values, which are the standard for quantifying an individual's exposure to radiation, were calculated for all scans performed. The effective dose was calculated by multiplying the DLP by a correction factor established by the ACR. The factor is 0.0023 for head scans and 0.015 for abdomen scans. The effective dose takes into account that different tissues are more radiosensitive than other tissues and that different types of radiation produce different biological effects. The effective dose values can be seen in Table 3.12

Table 3.12. Effective dose values, in mSv, for the 4, 16, and 64-slice Toshiba Aquillion® CT scanners.

	4-Slice (mSv)	16-Slice (mSv)	64-Slice (mSv)
Head Axial	1.28	0.90	0.84
Head Helical Set 1	2.87	1.75	2.01
Head Helical Set 2	1.80	1.10	1.27
Abdomen Axial	4.74	3.51	3.47
Abdomen Helical Set 1	5.56	3.15	4.06
Abdomen Helical Set 2	3.23	1.97	2.61

When comparing the effective dose values of the AA scans to those of the HA scans on all scanners, there was a decrease in exposure measurements of the head scans in relation to the abdomen scans. This is a complete reversal of what was previously seen in the exposure and DLP values. The head scans had the largest exposure values and DLP values but upon utilizing the weighting factor associated with the effective dose calculations, the abdomen scans produced the higher effective dose values in this study. This is a direct result of the fact that the tissues in the abdomen are overall more radiosensitive than tissues in the head. This fact reiterates why exposure values are not an accurate way to express dose from radiation exposure. The patterns seen in the previous data did continue in regards to the scanners slice capabilities and mode of scanning. The axial scans continued to display a reduction in dose as the slice capabilities of the

scanners increased. The percent decrease of the 16-slice relative to the 4-slice for the HA and AA scans was 30% (1.28 mSv vs. 0.90 mSv) and 26% (4.74 mSv vs. 3.51 mSv), respectively, and the percent decrease of the 64-slice relative to the 16-slice for the HA and AA scans was 7% (0.90 mSv vs. 0.84 mSv) and 1% (3.51 mSv vs. 3.47 mSv), respectively. The helical scans also did follow the patterns seen previously with all exposures of the 16-slice being less than those of the 4-slice and with all exposures from the 64-slice being higher than those of the 16-slice. The percent decrease was very uniform upon comparison of the 16-slice to the 4-slice, for the HH1, HH2 AH1 and AH2 scans the decreases were 39% (2.87 mSv vs. 1.75 mSv), 39% (1.8 mSv vs. 1.1 mSv), 43% (5.56 mSv vs. 3.15 mSv) and 39% (3.23 mSv vs. 1.97 mSv), respectively. The percent decrease of the 16-slice relative to the 64-slice for the HH1, HH2 AH1 and AH2 scans the decreases were 13% (2.01 mSv vs. 1.75 mSv), 13% (1.27 mSv vs. 1.1 mSv), 12% (4.06 mSv vs. 3.15 mSv) and 25% (2.61 mSv vs. 1.97 mSv), respectively.

CHAPTER 4

STUDY CONCLUSIONS

Over the past 30 years, rapid technological advances in CT have resulted in the number of scans being performed to increase annually, making it the major source of exposure to the population via diagnostic x-rays (Mettler et al. 2000). As the number of CT scans being performed has increased, so too has the concern over patient dose from CT (Mettler et al. 2000). CT contributes approximately 40% of the collective dose from diagnostic radiology to the general public even though it only accounts for about 5% of all the x-ray examinations (Kwan et al 1998). Due to their faster scan times at increased tube currents the multi-slice CT scanners have heightened the concern of dose in CT, and it is generally believed multi-slice scanners can lead to higher patient doses (Golding et al. 2002). This study's aim was to address these concerns by performing a dose comparison of three multi-slice CT scanners. All three scanners were the same make and model but varied in their slice capabilities, 4, 16, and 64-slice scanners were tested. Six protocols were utilized consisting of two axial protocols, one head and one abdomen, and four helical protocols, two head and two abdomen. All scan techniques were kept consistent for each scan performed on each scanner.

The $CTDI_{vol}$ values showed that the 4-slice scanner dose was the highest of any of the scanners for all of the protocols performed. Upon comparison of the 16-slice dose to the 64-slice, the 64-slice dose decreased for the two axial protocols but showed a slight

increase in the dose received during the helical protocols. The percent decrease in $CTDI_{vol}$ for the 16-slice to that of the 4-slice varied from 26% to 43%. The percent decrease in $CTDI_{vol}$ for the 64-slice to that of the 4-slice varied from 19% to 34%. The percent decreases in the axial scans $CTDI_{vol}$ for the 64-slice to that of the 16-slice were between 1 and 6% for the HA, and AA, respectively, while the helical scans $CTDI_{vol}$ values increased upon comparison of the 64-slice to the 16-slice scanner with a range of 13 to 33%.

The dose for the 16 and 64-slice axial scans were less than that of the 4-slice in all protocols used for the following reasons. For multi-slice CT scanners the nominal beam width is set to cover the entire area of the detectors with an added margin on both ends of the z-axis to account for penumbra and any mechanical errors (Mori et al. 2006). The exposure received in these margins does not add to the image quality but does add to the subject dose. As the nominal beam width enlarges, the effect on dose of these marginal exposures become less. This same effect holds true for the helical scans when comparing the 16 and 64-slice scanners to the 4-slice but does not hold true in this study upon comparison of the 16-slice to the 64-slice scanner. The increase in dose seen from the 16-slice to the 64-slice helical scans can be attributed to the interpolation phase of the helical image reconstruction, which necessitates added beam rotations outside of the volume of interest to allow reconstruction of the first and last image slices. Since the scan length for these protocols was of limited size, no greater than 15.5 cm, the extra revolutions needed by the 64-slice composed a larger area of the total volume imaged than that of the 16-slice. The exposures received due to this larger area outside the volume of interest outweighed the reduced exposure from the larger nominal beam width generating an

overall increase in dose. This effect should become less of a factor as the scan length increases, therefore, implying that smaller volumes should be imaged in either axial mode or 16-slice helical mode, rather than with 4-slice or 64-slice scanners.

The $CTDI_{vol}$ values were much higher for all the head protocols in comparison to the abdomen scans performed on the same scanners. This relationship was completely reversed upon calculation of effective dose values. The effective dose values take into account the overall increased radiosensitivity of the tissues in the abdomen as apposed to the tissues in the head producing numbers that gave a better reflection of the impact of the exposure to the imaged volume. We did continue to see the same pattern of decreased dose upon comparing the 16, and 64-slice scanners to the 4-slice for all protocols. The 64-slice axial scans continued the decrease when compared to the 16-slice axial scans but did show an increase in effective dose values for the helical scans in comparison to the 16-slice protocols. The effective dose values in this study ranged from 0.9 – 2.87 mSv for the head protocols and 1.97 – 5.56 mSv for the abdominal protocols. These values are the same magnitude as the average annual effective dose from background radiation in the United States (2.95 mSv) (Hall 2000). So on an individual basis the small dose differences between scanners is not so worrisome, but for the collective dose based on the thousands of CT scans being performed annually there is a significant impact.

The results of the dose comparison of the HH2 protocols utilizing three different pitch values showed there is a direct relationship between dose and pitch utilized in helical CT scanning. All exposures measured at a 1.4 pitch were exactly 50% of the exposures measured at a pitch of 0.7. Previous work has shown that CT scans utilizing pitch factors of up to 1.5 provide comparable image quality to scans performed at a pitch

factor of 1.0 in pediatric studies (Vade et al. 1996). With this in mind an obvious way to reduce dose while limiting the reduction of image quality is to increase the pitch. Image quality is always of the utmost importance in CT, but so should be the reduction of dose in the modality that produces approximately 40% of the collective dose from diagnostic radiology to the American population (Kwan et al 1998).

Standard CTDI calculation spreadsheets are utilized frequently to handle the laborious calculations involved in determining CT dose, but all are designed to estimate helical dose from axial scan exposures. This is a concern since in this study it was determined that there is an underestimation of dose when attempting to utilize axial data for helical dose calculations. The spreadsheets take into account the effect of the pitch in regards to the dose by dividing the $CTDI_w$ by the pitch factor used in the scan, but it does not take into account the extra revolutions needed by the helical scanners outside the imaged volume for the interpolation phase of image reconstruction. By not accounting for these extra revolutions an underestimation of dose ranging from 11% to 24% for the various scanners was produced. This sizable underestimation must be accounted for when performing dose calculations. There are methods to avoid this problem, but one must be aware when reviewing these records as to how the exposures were performed.

4.1 Overall Conclusions

With these conclusions comes a greater understanding of CT dose when comparing the newer scanners in use today. The biggest concern for increased dose from multi-slice CT scanners has commonly been attributed to the ease of use, i.e. faster scan times at increased tube outputs. This allows scans to be performed on patients that

previously would not have been candidates for CT scans, i.e. pediatric and elderly patients or anyone unable to hold still for minutes on end. This is still true, but by the results of this study, there must also be some thought process involved when ordering a CT scan as to which scanners should be utilized for various studies and types of patients. Pediatric patients should benefit the most from the information in this study because their smaller size generally infers that a smaller scan length is necessary and as we have determined here the optimum CT scanner would be a 16-slice for these individuals. I hope that the data presented here will aid health practitioners in deciding what CT studies and scanners should be utilized in various situations.

4.2 Future Work

Future research in this area could concentrate more on determining at what scan length does the dose from the 64-slice scanner become less than that of the 16-slice. In this study, the scan lengths were between 94 and 155 mm, which are not quite consistent with modern CT usage. Large portions of the CT scans performed today are for oncology purposes and generally consist of scanning the patient's neck, chest, abdomen and pelvis in one session. The dose from these longer length scans should be reduced by the use of the 64-slice models, but it would be of interest to determine at what length would the 64-slice scanner be the preferred scanner over the 16-slice. A 256-slice CT scanner has also been introduced into the market recently and the same questions could be raised regarding its use. The advertised use for these new units is as a cardiac screening tool but it would be interesting to perform a dose analysis for this type of scan. It would be very

unfortunate if in screening for cardiac disease the individual's likelihood of cancer could be increased.

APPENDIX A

CT Equipment Information

DEP Facility Number:			SDMI	
DEP Registration Number:			Facility Name	
Type:	Axial	x	Toshiba	
	Helical		CT Manufacturer	
	Total No. of Detectors	4	Jim Kelley	
Physicist's Name and Date Performed				

Ionization Chamber Instrumentation

Manufacturer and Model	Radcal 9095		
Last Date of Calibration	4/14/2006		
Active Chamber Length (L) (mm)	100		
Chamber Correction Factor (C)	1		

Patient Scan Protocol

Procedure Type:		Head	
kVp	120	Procedures Types Not Performed By Facility	
mA	200		
Exposure time per rotation	1		
Z axis collimation (T) (mm)	1.00		
# of data channels used (N)	96		
If Axial: Table Increment (I) (mm)			
OR		96.00	
If Helical: Table Speed (I) (mm/rot)			

Scan Measurements

At Isocenter of Phantom			
1st Measurement (mR)*	5849.0		
2nd Measurement (mR)*	5849.0		
3rd Measurement (mR)*	5849.0		
Average Measurement (mR)	5849.0	CTDI_{ref} at isocenter (mGy)	53.01
* Measurements must be w/i 5% of each other			
At 12 o'clock Position of Phantom			
1st Measurement (mR)*	6692.0	CTDI_{ref} at 12 o'clock (mGy)	60.95
2nd Measurement (mR)*	6692.0		
3rd Measurement (mR)*	6692.0		
Average Measurement (mR)	6692.0		

CT Dose Calculations and Pitch

CTDI_w (mGy)	58.10	CTDI_{vol} (mGy)	58.10
Pitch	1.000		

CT Equipment Information

DEP Facility Number:		SDMI
DEP Registration Number:		Facility Name
Type:	Axial	Toshiba
	Helical	CT Manufacturer
	x	Jim Kelley
Total No. of Detectors	4	Physicist's Name and Date Performed

Ionization Chamber Instrumentation

Manufacturer and Model	Radcal 9095	
Last Date of Calibration	4/14/2006	
Active Chamber Length (L) (mm)	100	
Chamber Correction Factor (C)	1	

Patient Scan Protocol

Procedure Type:	Head	
kVp	120	Procedures Types Not Performed By Facility
mA	300	
Exposure time per rotation	1	
Z axis collimation (T) (mm)	1.00	
# of data channels used (N)	154	
If Axial: Table Increment (I) (mm)		
OR	136.00	
If Helical: Table Speed (I) (mm/rot)		

Scan Measurements

At Isocenter of Phantom			
1st Measurement (mR)*	11879.0		
2nd Measurement (mR)*	11879.0		
3rd Measurement (mR)*	11879.0		
Average Measurement (mR)	11879.0	CT DI at Isocenter (mGy)	67.11
At 12 o'clock Position of Phantom			
		* Measurements must be w/i 5% of each other	
1st Measurement (mR)*	13055.0	CT DI at 12 o'clock (mGy)	73.75
2nd Measurement (mR)*	13055.0		
3rd Measurement (mR)*	13055.0		
Average Measurement (mR)	13055.0		

CT Dose Calculations and Pitch

CT DI_{ax} (mGy)	71.54	CT DI_{12o} (mGy)	81.01
Pitch	0.883		

CT Equipment Information

DEP Facility Number:		SDMI
DEP Registration Number:		Facility Name
Type:	Axial	Toshiba
	Helical	CT Manufacturer
	x	Jim Kelley
Total No. of Detectors	4	Physicist's Name and Date Performed

Ionization Chamber Instrumentation

Manufacturer and Model	Radcal 9095	
Last Date of Calibration	4/14/2006	
Active Chamber Length (L) (mm)	100	
Chamber Correction Factor (C)	1	

Patient Scan Protocol

Procedure Type:	Head	
kVp	120	Procedures Types Not Performed By Facility
mA	200	
Exposure time per rotation	1	
Z axis collimation (T) (mm)	1.00	
# of data channels used (N)	98	
If Axial: Table Increment (I) (mm) OR	86.00	
If Helical: Table Speed (I) (mm/rot)		

Scan Measurements

At isocenter of Phantom			
1st Measurement (mR)*	7298.0		
2nd Measurement (mR)*	7298.0		
3rd Measurement (mR)*	7298.0		
Average Measurement (S) (mR)	7298.0	CTDI _{iso} at isocenter (mGy)	64.79
At 12 o'clock Position of Phantom			
		* Measurements must be w/i 5% of each other	
1st Measurement (mR)*	8164.0	CTDI _{no} at 12 o'clock (mGy)	72.48
2nd Measurement (mR)*	8164.0		
3rd Measurement (mR)*	8164.0		
Average Measurement (S) (mR)	8164.0		

CT Dose Calculations and Pitch

CTDI _{vol} (mGy)	69.92	CTDI _{vol} (mGy)	79.67
Pitch	0.878		

CT Equipment Information

DEP Facility Number:		SDMI
DEP Registration Number:		Facility Name
Type:	Axial	Toshiba
	Helical	CT Manufacturer
	Total No. of Detectors	Jim Kelley
	4	Physicist's Name and Date Performed

Ionization Chamber Instrumentation

Manufacturer and Model	Radcal 9095	
Last Date of Calibration	4/14/2006	
Active Chamber Length (L) (mm)	100	
Chamber Correction Factor (C)	1	

Patient Scan Protocol

Procedure Type:	Abdomen	
kVp	120	Procedures Types Not Performed By Facility
mA	200	
Exposure time per rotation	1	
Z axis collimation (T) (mm)	1.00	
# of data channels used (N)	96	
If Axial: Table Increment (I) (mm) OR	96.00	
If Helical: Table Speed (I) (mm/rot)		

Scan Measurements

At Isocenter of Phantom			
1st Measurement (mR)*	2086.0		
2nd Measurement (mR)*	2086.0		
3rd Measurement (mR)*	2086.0		
Average Measurement (E) (mR)	2086.0	CTDI _{ref} at Isocenter (mGy)	18.90
At 12 o'clock Position of Phantom			
		* Measurements must be w/i 5% of each other	
1st Measurement (mR)*	4400.00	CTDI _{ref} at 12 o'clock (mGy)	39.88
2nd Measurement (mR)*	4400.00		
3rd Measurement (mR)*	4400.00		
Average Measurement (E) (mR)	4400.00		

CT Dose Calculations and Pitch

CTDI _w (mGy)	32.89	CTDI _{vol} (mGy)	32.89
Pitch	1.000		

CT Equipment Information

DEP Facility Number:		SDMI
DEP Registration Number:		Facility Name
Type:	Axial	Toshiba
	Helical	CT Manufacturer
	Total No. of Detectors	Jim Kelley
		Physicist's Name and Date Performed

Ionization Chamber Instrumentation

Manufacturer and Model	Radcal 9095	
Last Date of Calibration	4/14/2006	
Active Chamber Length (L) (mm)	100	
Chamber Correction Factor (C)	1	

Patient Scan Protocol

Procedure Type:	Abdomen	
kVp	120	Procedures Types Not Performed By Facility
mA	300	
Exposure time per rotation	0.5	
Z axis collimation (T) (mm)	1.00	
# of data channels used (N)	154	
If Axial: Table Increment (I) (mm) OR If Helical: Table Speed (I) (mm/rot)	135.00	

Scan Measurements

At isocenter of Phantom			
1st Measurement (mR)*	2318.0		
2nd Measurement (mR)*	2318.0		
3rd Measurement (mR)*	2318.0		
Average Measurement (E) (mR)	2318.0	CTDI _{vol} at isocenter (mGy)	13.10
At 12 o'clock Position of Phantom			
		* Measurements must be w/i 5% of each other	
1st Measurement (mR)*	4437.0	CTDI _{max} at 12 o'clock (mGy)	25.07
2nd Measurement (mR)*	4437.0		
3rd Measurement (mR)*	4437.0		
Average Measurement (E) (mR)	4437.0		

CT Dose Calculations and Pitch

CTDI _{vol} (mGy)	21.08	CTDI _{vol} (mGy)	24.05
Pitch	0.877		

CT Equipment Information

DEP Facility Number:		SDMI
DEP Registration Number:		Facility Name
Type:	Axial	Toshiba
	Helical	CT Manufacturer
	Total No. of Detectors	Jim Kelley
		Physicist's Name and Date Performed

Ionization Chamber Instrumentation

Manufacturer and Model	Radcal 9095	
Last Date of Calibration	4/14/2006	
Active Chamber Length (L) (mm)	100	
Chamber Correction Factor (C)	1	

Patient Scan Protocol

Procedure Type:	Abdomen	
kVp	120	Procedures Types Not Performed By Facility
mA	200	
Exposure time per rotation	0.5	
Z axis collimation (T) (mm)	1.00	
# of data channels used (N)	98	
If Axial: Table Increment (I) (mm)		
OR	86.00	
If Helical: Table Speed (I) (mm/rot)		

Scan Measurements

At Isocenter of Phantom			
1st Measurement (mR)*	1276.0		
2nd Measurement (mR)*	1276.0		
3rd Measurement (mR)*	1276.0		
Average Measurement (E) (mR)	1276.0	CTDI_W at isocenter (mGy)	11.33
At 12 o'clock Position of Phantom			
		* Measurements must be w/i 5% of each other	
1st Measurement (mR)*	2617.0	CTDI_W at 12 o'clock (mGy)	23.23
2nd Measurement (mR)*	2617.0		
3rd Measurement (mR)*	2617.0		
Average Measurement (E) (mR)	2617.0		

CT Dose Calculations and Pitch

CTDI_W (mGy)	19.27	CTDI_{Vol} (mGy)	21.96
Pitch	0.878		

CT Equipment Information

DEP Facility Number:		SDMI
DEP Registration Number:		Facility Name
Type:	Axial	Toshiba
	Helical	CT Manufacturer
	Total No. of Detectors	Jim Kelley
	16	Physicist's Name and Date Performed

Ionization Chamber Instrumentation

Manufacturer and Model	Radcal 9095	
Last Date of Calibration	4/14/2006	
Active Chamber Length (L) (mm)	100	
Chamber Correction Factor (C)	1	

Patient Scan Protocol

Procedure Type:	Head	
kVp	120	Procedures Types Not Performed By Facility
mA	200	
Exposure time per rotation	1	
Z axis collimation (T) (mm)	1.00	
# of data channels used (N)	96	
If Axial:Table Increment (I)(mm)		
OR	96.00	
If Helical:Table Speed (I) (mm/rot)		

Scan Measurements

At Isocenter of Phantom			
1st Measurement (mR)*	4105.0		
2nd Measurement (mR)*	4105.0		
3rd Measurement (mR)*	4105.0		
Average Measurement (E) (mR)	4105.0	CTDI₁₀₀ at Isocenter (mGy)	37.20
At 12 o'clock Position of Phantom			
		* Measurements must be w/i 5% of each other	
1st Measurement (mR)*	4677.0	CTDI₁₀₀ at 12 o'clock (mGy)	42.39
2nd Measurement (mR)*	4677.0		
3rd Measurement (mR)*	4677.0		
Average Measurement (E) (mR)	4677.0		

CT Dose Calculations and Pitch

CTDI_w (mGy)	40.66	CTDI_{vol} (mGy)	40.66
Pitch	1.000		

CT Equipment Information

DEP Facility Number:		SDMI
DEP Registration Number:		Facility Name
Type:	Axial	Toshiba
	Helical	CT Manufacturer
	x	Jim Kelley
Total No. of Detectors	16	Physicist's Name and Date Performed

Ionization Chamber Instrumentation

Manufacturer and Model	Radcal 9095	
Last Date of Calibration	4/14/2006	
Active Chamber Length (L) (mm)	100	
Chamber Correction Factor (C)	1	

Patient Scan Protocol

Procedure Type:	Head	
kVp	120	Procedures Types Not Performed By Facility
mA	300	
Exposure time per rotation	1	
Z axis collimation (T) (mm)	1.00	
# of data channels used (N)	154	
If Axial: Table Increment (I) (mm)		
OR	144.00	
If Helical: Table Speed (I) (mm/rot)		

Scan Measurements

At Isocenter of Phantom			
1st Measurement (mR)*	7802.0		
2nd Measurement (mR)*	7802.0		
3rd Measurement (mR)*	7802.0		
Average Measurement (5) (mR)	7802.0	CTDI_{iso} at isocenter (mGy)	44.08
At 12 o'clock Position of Phantom		* Measurements must be w/i 5% of each other	
1st Measurement (mR)*	8342.0	CTDI_{max} at 12 o'clock (mGy)	47.13
2nd Measurement (mR)*	8342.0		
3rd Measurement (mR)*	8342.0		
Average Measurement (5) (mR)	8342.0		

CT Dose Calculations and Pitch

CTDI_w (mGy)	46.11	CTDI_{vol} (mGy)	49.31
Pitch	0.935		

CT Equipment Information

DEP Facility Number:		SDMI
DEP Registration Number:		Facility Name
Type:	Axial	Toshiba
	Helical	CT Manufacturer
		Jim Kelley
Total No. of Detectors	16	Physicist's Name and Date Performed

Ionization Chamber Instrumentation

Manufacturer and Model	Radcal 9095	
Last Date of Calibration	4/14/2006	
Active Chamber Length (L) (mm)	100	
Chamber Correction Factor (C)	1	

Patient Scan Protocol

Procedure Type:	Head	
kVp	120	Procedures Types Not Performed
mA	200	
Exposure time per rotation	1	
Z axis collimation (T) (mm)	1.00	
# of data channels used (N)	98	
If Axial: Table Increment (I) (mm)		
OR	92.00	By Facility
If Helical: Table Speed (I) (mm/rot)		

Scan Measurements

At Isocenter of Phantom			
1st Measurement (mR)*	4871.0		
2nd Measurement (mR)*	4871.0		
3rd Measurement (mR)*	4871.0		
Average Measurement (mR)	4871.0	Calculated Exposure (mGy)	43.24
At 12 o'clock Position of Phantom			
		* Measurements must be w/i 5% of each other	
1st Measurement (mR)*	5333.0	Calculated Exposure (mGy)	47.34
2nd Measurement (mR)*	5333.0		
3rd Measurement (mR)*	5333.0		
Average Measurement (mR)	5333.0		

CT Dose Calculations and Pitch

CTDI_{vol} (mGy)	45.98	CTDI_{vol} (mGy)	48.98
Pitch	0.939		

CT Equipment Information

DEP Facility Number:		SDMI
DEP Registration Number:		Facility Name
Type:	Axial	Toshiba
	Helical	CT Manufacturer
	Total No. of Detectors	Jim Kelley
	16	Physicist's Name and Date Performed

Ionization Chamber Instrumentation

Manufacturer and Model	Radcal 9095	
Last Date of Calibration	4/14/2006	
Active Chamber Length (L) (mm)	100	
Chamber Correction Factor (C)	1	

Patient Scan Protocol

Procedure Type:	Abdomen	
kVp	120	Procedures Types Not Performed By Facility
mA	200	
Exposure time per rotation	1	
Z axis collimation (T) (mm)	1.00	
# of data channels used (N)	96	
if Axial: Table Increment (I) (mm)		
OR	96.00	
If Helical: Table Speed (I) (mm/rot)		

Scan Measurements

At isocenter of Phantom			
1st Measurement (mR)*	1429.0		
2nd Measurement (mR)*	1429.0		
3rd Measurement (mR)*	1429.0		
Average Measurement (mR)	1429.0	CTDI Head (mG)	12.95
At 12 o'clock Position of Phantom			
		* Measurements must be w/ 5% of each other	
1st Measurement (mR)*	3324.0	CTDI Head (mG)	30.12
2nd Measurement (mR)*	3324.0		
3rd Measurement (mR)*	3324.0		
Average Measurement (mR)	3324.0		

CT Dose Calculations and Pitch

CTDI (mG)	24.40	CTDI (mG)	24.40
Pitch	1.000		

CT Equipment Information

DEP Facility Number:		SDMI
DEP Registration Number:		Facility Name
Type:	Axial	Toshiba
	Helical	CT Manufacturer
	Total No. of Detectors	Jim Kelley
		Physicist's Name and Date Performed

Ionization Chamber Instrumentation

Manufacturer and Model	Radcal 9095	
Last Date of Calibration	4/14/2006	
Active Chamber Length (L) (mm)	100	
Chamber Correction Factor (C)	1	

Patient Scan Protocol

Procedure Type:	Abdomen	
kVp	120	Procedures Types Not Performed By Facility
mA	300	
Exposure time per rotation	1	
Z axis collimation (T) (mm)	1.00	
# of data channels used (N)	154	
If Axial: Table Increment (I) (mm)		
OR	144.00	
If Helical: Table Speed (I) (mm/rot)		

Scan Measurements

At Isocenter of Phantom			
1st Measurement (mR)*	1546.0		
2nd Measurement (mR)*	1546.0		
3rd Measurement (mR)*	1546.0		
Average Measurement (Σ) (mR)	1546.0	CTDI₁₀₀ at Isocenter (mGy)	8.73
At 12 o'clock Position of Phantom			
		* Measurements must be w/i 5% of each other	
1st Measurement (mR)*	2611.0	CTDI_{max} at 12 o'clock (mGy)	14.75
2nd Measurement (mR)*	2611.0		
3rd Measurement (mR)*	2611.0		
Average Measurement (Σ) (mR)	2611.0		

CT Dose Calculations and Pitch

CTDI_w (mGy)	12.75	CTDI_{vol} (mGy)	13.63
Pitch	0.935		

CT Equipment Information

DEP Facility Number:		SDMI
DEP Registration Number:		Facility Name
Type:	Axial	Toshiba
	Helical	CT Manufacturer
	x	Jim Kelley
Total No. of Detectors	16	Physicist's Name and Date Performed

Ionization Chamber instrumentation

Manufacturer and Model	Radcal 9095	
Last Date of Calibration	4/14/2006	
Active Chamber Length (L) (mm)	100	
Chamber Correction Factor (C)	1	

Patient Scan Protocol

Procedure Type:	Abdomen	
kVp	120	Procedures Types Not Performed By Facility
mA	200	
Exposure time per rotation	0.5	
Z axis collimation (T) (mm)	1.00	
# of data channels used (N)	98	
If Axial:Table Increment (I)(mm)		
OR	92.00	
If Helical:Table Speed (I) (mm/rot)		

Scan Measurements

At Isocenter of Phantom			
1st Measurement (mR)*	924.0		
2nd Measurement (mR)*	924.0		
3rd Measurement (mR)*	924.0		
Average Measurement (C) (mR)	924.0	CTDI (mR) at isocenter (mG)	8.20
At 12 o'clock Position of Phantom			
		* Measurements must be w/i 5% of each other	
1st Measurement (mR)*	1664.0	CTDI (mR) at 12 o'clock (mG)	14.77
2nd Measurement (mR)*	1664.0		
3rd Measurement (mR)*	1664.0		
Average Measurement (C) (mR)	1664.0		

CT Dose Calculations and Pitch

CTDI (mG)	12.58	CTDI (mG)	13.41
Pitch	0.939		

CT Equipment Information

DEP Facility Number:		SDMI
DEP Registration Number:		Facility Name
Type:	x	Toshiba
		CT Manufacturer
Total No. of Detectors	64	Jim Kelley
		Physicist's Name and Date Performed

Ionization Chamber Instrumentation

Manufacturer and Model	Radcal 9095	
Last Date of Calibration	4/14/2006	
Active Chamber Length (L) (mm)	100	
Chamber Correction Factor (C)	1	

Patient Scan Protocol

Procedure Type:	Head	
kVp	120	Procedures Types Not Performed By Facility
mA	200	
Exposure time per rotation	1	
Z axis collimation (T) (mm)	1.00	
# of data channels used (N)	96	
If Axial: Table Increment (I) (mm) OR	96.00	
If Helical: Table Speed (I) (mm/rot)		

Scan Measurements

At Isocenter of Phantom			
1st Measurement (mR)*	3819.0		
2nd Measurement (mR)*	3819.0		
3rd Measurement (mR)*	3819.0		
Average Measurement (3 mR)	3819.0	CTDI at Isocenter (mGy)	34.61
At 12 o'clock Position of Phantom			
		* Measurements must be w/i 5% of each other	
1st Measurement (mR)*	4423.0	CTDI at 12 o'clock (mGy)	40.08
2nd Measurement (mR)*	4423.0		
3rd Measurement (mR)*	4423.0		
Average Measurement (3 mR)	4423.0		

CT Dose Calculations and Pitch

CT DI (mGy)	38.26	CT DI (mGy)	38.26
Pitch	1.000		

CT Equipment Information

DEP Facility Number:		SDMI
DEP Registration Number:		Facility Name
Type:	Axial	Toshiba
	Helical	CT Manufacturer
	x	Jim Kelley
Total No. of Detectors	64	Physicist's Name and Date Performed

Ionization Chamber Instrumentation

Manufacturer and Model	Radcal 9095	
Last Date of Calibration	4/14/2006	
Active Chamber Length (L) (mm)	100	
Chamber Correction Factor (C)	1	

Patient Scan Protocol

Procedure Type:	Head	
kVp	120	Procedures Types Not Performed By Facility
mA	300	
Exposure time per rotation	1	
Z axis collimation (T) (mm)	1.00	
# of data channels used (N)	155	
If Axial: Table Increment (I) (mm)		
OR	141.00	
If Helical: Table Speed (I) (mm/rot)		

Scan Measurements

At Isocenter of Phantom			
1st Measurement (mR)*	8624.0		
2nd Measurement (mR)*	8624.0		
3rd Measurement (mR)*	8624.0		
Average Measurement (mR)	8624.0	CT DI at Isocenter (mGy)	48.41
At 12 o'clock Position of Phantom		* Measurements must be w/i 5% of each other	
1st Measurement (mR)*	9407.0	CT DI at 12 o'clock (mGy)	52.80
2nd Measurement (mR)*	9407.0		
3rd Measurement (mR)*	9407.0		
Average Measurement (mR)	9407.0		

CT Dose Calculations and Pitch

CT DI (mGy)	51.34	CT DI w/d (mGy)	56.43
Pitch	0.910		

CT Equipment Information

DEP Facility Number:		SDMI
DEP Registration Number:		Facility Name
Type:	Axial	Toshiba
	Helical	CT Manufacturer
		Jim Kelley
Total No. of Detectors	64	Physicist's Name and Date Performed

Ionization Chamber Instrumentation

Manufacturer and Model	Radcal 9095	
Last Date of Calibration	4/14/2006	
Active Chamber Length (L) (mm)	100	
Chamber Correction Factor (C)	1	

Patient Scan Protocol

Procedure Type:	Head	
kVp	120	Procedures Types Not Performed By Facility
mA	200	
Exposure time per rotation	1	
Z axis collimation (T) (mm)	1.00	
# of data channels used (N)	100	
If Axial: Table Increment (I) (mm)		
OR	91.00	
If Helical: Table Speed (I) (mm/rot)		

Scan Measurements

At Isocenter of Phantom			
1st Measurement (mR)*	5522.0		
2nd Measurement (mR)*	5522.0		
3rd Measurement (mR)*	5522.0		
Average Measurement (E) (mR)	5522.0	CTDI₁₀₀ at Isocenter (mGy)	48.04
At 12 o'clock Position of Phantom			
* Measurements must be w/i 5% of each other			
1st Measurement (mR)*	5895.0	CTDI₁₀₀ at 12 o'clock (mGy)	51.29
2nd Measurement (mR)*	13055.0		
3rd Measurement (mR)*	13055.0		
Average Measurement (E) (mR)	13055.0		

CT Dose Calculations and Pitch

CTDI_w (mGy)	50.21	CTDI_{vol} (mGy)	55.17
Pitch	0.910		

CT Equipment Information

DEP Facility Number:			SDMI	
DEP Registration Number:			Facility Name	
Type:	Axial	x	Toshiba	
	Helical		CT Manufacturer	
	Total No. of Detectors	64	Jim Kelley	
Physicist's Name and Date Performed				

Ionization Chamber Instrumentation

Manufacturer and Model	Radcal 9095		
Last Date of Calibration	4/14/2006		
Active Chamber Length (L) (mm)	100		
Chamber Correction Factor (C)	1		

Patient Scan Protocol

Procedure Type:		Abdomen		
kVp	120	Procedures Types Not Performed	By Facility	
mA	200			
Exposure time per rotation	1			
Z axis collimation (T) (mm)	1.00			
# of data channels used (N)	96			
If Axial:Table Increment (I)(mm)				
OR	96.00			
If Helical:Table Speed (I) (mm/rot)				

Scan Measurements

At Isocenter of Phantom			
1st Measurement (mR)*	1252.0		
2nd Measurement (mR)*	1252.0		
3rd Measurement (mR)*	1252.0		
Average Measurement (E) (mR)	1252.0	CTDI_{vol} at isocenter (mGy)	11.35
At 12 o'clock Position of Phantom		* Measurements must be w/i 5% of each other	
1st Measurement (mR)*	3364.0	CTDI_{vol} at 12 o'clock (mGy)	30.49
2nd Measurement (mR)*	3364.0		
3rd Measurement (mR)*	3364.0		
Average Measurement (E) (mR)	3364.0		

CT Dose Calculations and Pitch

CTDI_W (mGy)	24.11	CTDI_{vol} (mGy)	24.11
Pitch	1.000		

CT Equipment Information

DEP Facility Number:		SDMI
DEP Registration Number:		Facility Name
Type:	Axial	Toshiba
	Helical	CT Manufacturer
		Jim Kelley
Total No. of Detectors	64	Physicist's Name and Date Performed

Ionization Chamber Instrumentation

Manufacturer and Model	Radcal 9095	
Last Date of Calibration	4/14/2006	
Active Chamber Length (L) (mm)	100	
Chamber Correction Factor (C)	1	

Patient Scan Protocol

Procedure Type:	Abdomen	
kVp	120	Procedures Types Not Performed By Facility
mA	300	
Exposure time per rotation	0.5	
Z axis collimation (T) (mm)	1.00	
# of data channels used (N)	154	
If Axial: Table Increment (I) (mm) OR	140.00	
If Helical: Table Speed (I) (mm/rot)		

Scan Measurements

At isocenter of Phantom			
1st Measurement (mR)*	1890.0		
2nd Measurement (mR)*	1890.0		
3rd Measurement (mR)*	1890.0		
Average Measurement (E) (mR)	1890.0	CT DI at Isocenter (mGy)	10.68
At 12 o'clock Position of Phantom			
		* Measurements must be w/i 5% of each other	
1st Measurement (mR)*	3297.0.0	CT DI at 12 o'clock (mGy)	18.63
2nd Measurement (mR)*	3297.0.0		
3rd Measurement (mR)*	3297.0.0		
Average Measurement (E) (mR)	3297.0.0		

CT Dose Calculations and Pitch

CT DI (mGy)	15.98	CT DI at 12 o'clock (mGy)	17.58
Pitch	0.909		

CT Equipment Information

DEP Facility Number:			SDMI	
DEP Registration Number:			Facility Name	
Type:	Axial		Toshiba	
	Helical	x	CT Manufacturer	
	Total No. of Detectors	64	Jim Kelley	
Physicist's Name and Date Performed				

Ionization Chamber Instrumentation

Manufacturer and Model	Radcal 9095		
Last Date of Calibration	4/14/2006		
Active Chamber Length (L) (mm)	100		
Chamber Correction Factor (C)	1		

Patient Scan Protocol

Procedure Type:	Abdomen		
kVp	120	Procedures Types Not Performed By Facility	
mA	200		
Exposure time per rotation	0.5		
Z axis collimation (T) (mm)	1.0		
# of data channels used (N)	97		
If Axial: Table Increment (I) (mm)			
OR	89.00		
If Helical: Table Speed (I) (mm/rot)			

Scan Measurements

At isocenter of Phantom			
1st Measurement (mR)*	1185.0		
2nd Measurement (mR)*	1185.0		
3rd Measurement (mR)*	1185.0		
Average Measurement (mR)	1185.0	CT DI at isocenter (mGy)	10.52
* Measurements must be w/i 5% of each other			
At 12 o'clock Position of Phantom			
1st Measurement (mR)*	2137.0	CT DI at 12 o'clock (mGy)	18.97
2nd Measurement (mR)*	2137.0		
3rd Measurement (mR)*	2137.0		
Average Measurement (mR)	2137.0		

CT Dose Calculations and Pitch

CT DI (mGy)	16.16	CT DI at isocenter (mGy)	17.79
Pitch	0.908		

APPENDIX B

CT Equipment Information

DEP Facility Number:		SDMI
DEP Registration Number:		Facility Name
Type:	Axial	Toshiba
	Helical	CT Manufacturer
	Total No. of Detectors	Jim Kelley
		Physicist's Name and Date Performed

Ionization Chamber instrumentation

Manufacturer and Model	Radcal 9095	
Last Date of Calibration	4/14/2006	
Active Chamber Length (L) (mm)	100	
Chamber Correction Factor (C)	1	

Patient Scan Protocol

Procedure Type:	Head	
kVp	120	Procedures Types Not Performed By Facility
mA	200	
Exposure time per rotation	1.0	
Z axis collimation (T) (mm)	1.00	
# of data channels used (N)	96	
If Axial: Table Increment (I) (mm)		
OR	84.25	
If Helical: Table Speed (I) (mm/rot)		

Scan Measurements

At isocenter of Phantom			
1st Measurement (mR)*	5849.0		
2nd Measurement (mR)*	5849.0		
3rd Measurement (mR)*	5849.0		
Average Measurement (E) (mR)	5849.0	CTDI _W at isocenter (mGy)	53.01
At 12 o'clock Position of Phantom			
		* Measurements must be w/i 5% of each other	
1st Measurement (mR)*	6692.0	CTDI _W at 12 o'clock (mGy)	60.65
2nd Measurement (mR)*	6692.0		
3rd Measurement (mR)*	6692.0		
Average Measurement (E) (mR)	6692.0		

CT Dose Calculations and Pitch

CTDI _W (mGy)	58.10	CTDI _{vol} (mGy)	66.21
Pitch	0.878		

CT Equipment Information

DEP Facility Number:		SDMI
DEP Registration Number:		Facility Name
Type:	Axial	Toshiba
	Helical	CT Manufacturer
	x	Jim Kelley
Total No. of Detectors	16	Physicist's Name and Date Performed

Ionization Chamber Instrumentation

Manufacturer and Model	Radcal 9095	
Last Date of Calibration	4/14/2006	
Active Chamber Length (L) (mm)	100	
Chamber Correction Factor (C)	1	

Patient Scan Protocol

Procedure Type:	Head				
kVp	120	<table border="1" style="width: 100%; border-collapse: collapse;"> <tr> <td style="text-align: center;">Procedures Types Not Performed</td> </tr> <tr> <td style="text-align: center;">By Facility</td> </tr> <tr> <td style="height: 20px;"></td> </tr> </table>	Procedures Types Not Performed	By Facility	
Procedures Types Not Performed					
By Facility					
mA	200				
Exposure time per rotation	1				
Z axis collimation (T) (mm)	1.00				
# of data channels used (N)	96				
If Axial: Table Increment (I) (mm)					
OR	90.10				
if Helical: Table Speed (I) (mm/rot)					

Scan Measurements

At Isocenter of Phantom			
1st Measurement (mR)*	4105.0		
2nd Measurement (mR)*	4105.0		
3rd Measurement (mR)*	4105.0		
Average Measurement (E) (mR)	4105.0	Average Measurement (E) (mSv)	37.20
At 12 o'clock Position of Phantom		* Measurements must be w/i 5% of each other	
1st Measurement (mR)*	4677.0	Average Measurement (E) (mSv)	42.39
2nd Measurement (mR)*	4677.0		
3rd Measurement (mR)*	4677.0		
Average Measurement (E) (mR)	4677.0		

CT Dose Calculations and Pitch

Ct DI (mSv)	40.66	Ct DI (mSv)	43.32
Pitch	0.939		

CT Equipment Information

DEP Facility Number:		SDMI
DEP Registration Number:		Facility Name
Type:	Axial	Toshiba
	Helical	CT Manufacturer
	Total No. of Detectors	Jim Kelley
		Physicist's Name and Date Performed

Ionization Chamber instrumentation

Manufacturer and Model	Radcal 9095	
Last Date of Calibration	4/14/2006	
Active Chamber Length (L) (mm)	100	
Chamber Correction Factor (C)	1	

Patient Scan Protocol

Procedure Type:	Head	
kVp	120	Procedures Types Not Performed By Facility
mA	200	
Exposure time per rotation	1	
Z axis collimation (T) (mm)	1.00	
# of data channels used (N)	96	
If Axial:Table Increment (I)(mm)		
OR	87.40	
If Helical:Table Speed (I) (mm/rot)		

Scan Measurements

At Isocenter of Phantom			
1st Measurement (mR)*	3819.0		
2nd Measurement (mR)*	3819.0		
3rd Measurement (mR)*	3819.0		
Average Measurement (mR)	3819.0	CT DI at isocenter (mGy)	34.61
At 12 o'clock Position of Phantom			
		* Measurements must be w/i 5% of each other	
1st Measurement (mR)*	4423.0		
2nd Measurement (mR)*	4423.0		
3rd Measurement (mR)*	4423.0		
Average Measurement (mR)	4423.0		

CT Dose Calculations and Pitch

CT DI (mGy)	38.26	CT DI at isocenter (mGy)	42.03
Pitch	0.910		

BIBLIOGRAPHY

- Bushberg JT, Siebert JA, Liedholt EM, Boone JM. The Essential Physics of Medical Imaging. Philadelphia, PA: Lippincott Williams & Wilkins; 2002: 747-759.
- Brunnett CJ. CT design considerations and specifications. Cleveland, Ohio. Picker International; 1990.
- Cardinal Health. Instruction Manual for CT Head and Body Dose Phantom Model Number 76-414-4150; 1991.
- Dawson P, Lees WR. Multi-slice technology in computed tomography. *Clinical Radiology* 56: 302-309; 1990.
- Feldkamp LA, Davis LC, Kress JW. Practical cone-beam algorithm. *Journal Opt. Soc. Am. A* 1: 612-619; 1984.
- Food and Drug Administration. Code of Federal Regulations; Title 21 Part 1020 Section 33; 2003. Available at: <http://frwebgocite.access.gpo.gov/cgi-bin/get-cfr.cgi>. Accessed 19 July 2006.
- Golding SJ, Shrimpton PC. Radiation dose in CT: are we meeting the challenge? *British Journal of Radiology* 75: 1-4; 2002.
- Hall EJ. Radiobiology for the Radiologist. Philadelphia, PA: Lippincott Williams & Wilkins; 2000: 234-248.
- Hu H. Multislice Helical CT: Scan and Reconstruction. *Med Physics* 26: 5-18; 1999.
- Jessen KA, Shrimpton PC, Geleijns J, Panzer W, Tosi G. Dosimetry for optimization of patient protection in computed tomography. *Applied Radiation and Isotopes* 50: 165-172; 1999.
- Jucius RA, Kambic GX. Radiation dosimetry in computed tomography. *Appl. Opt. Instrum. Eng. Med.* 127: 286-295; 1977.
- Lewis M. Radiation Dose Issues in Multi-Slice CT Scanning. 2005. Available at: <http://www.impactscan.org/msctdose.htm>. Accessed 10 May 2006.
- Mettler FA, Wiest P, Locken JA. CT scanning: Patterns of Use and Dose. *Radiol. Prot.* 20: 353-359; 2000.
- Morgan CL. Basic Principles of Computed Tomography. Baltimore, MD; University Park Press; 1983: 51-68.
- Mori S, Endo M, Nishizawa K, Murase K, Fujiwara H, Tanada S. Comparison of patient doses in 256-slice CT and 16-slice CT scanners. *British Journal of Radiology* 79: 56-61; 2006.
- Ng KH, Bradley DA. Warren-forward, H.M. Subject Dose in Radiological Imaging New York, NY; Elsevier; 1998: 165-172.
- Nicholson R, Fetherston S. Primary Radiation Outside the Imaged Volume of a Multi-slice Helical CT Scan. *British Journal of Radiology* 75: 518-522; 2002.
- Radcal . 9095 Technical Specifications Brochure. 2005. Available at: <http://www.radcal.com/9095.html>. Accessed 12 July 2006.
- Saito Y. Multislice X-ray CT Scanner. *Med Rev.* 66: 1-8; 1998.

- Seeram E. Computed Tomography Physical Principals, Clinical Applications and Quality Control, 2nd Ed.. Philadelphia, PA: Saunders; 2001: 245-265.
- Vade A, Demos TC, Olson MC, Subbaiah P, Turbin RC, Vickery K, Carrigan K. Evaluation of image quality using 1:1 pitch and 1.5:1 pitch helical CT in children: a comparative study. Pediatric Radiology 26: 891-893; 1996.

VITA

Graduate College
University of Nevada, Las Vegas

James J. Kelley

Home Address:

284 Ben Johnson Ct.
Las Vegas, Nevada 89123

Degrees:

Bachelor of Science, Nuclear Medicine, 1988
University of Nevada, Las Vegas

Thesis Title: Dose Comparison of Multi-Slice Computed Tomography Scanners

Thesis Examination Committee:

Chairperson, Dr. Phillip Patton, Ph.D.
Committee Member, Dr. Steen Madsen, Ph.D.
Committee Member, Dr. Mark Rudin, Ph.D.
Graduate Faculty Representative, Dr. J. Wesley McWhorter, Ph.D.